A simple and efficient method for polymer coating of iron oxide nanoparticles

Ahmed Abushrida[1], Ibteisam Elhuni[1], Vincenzo Taresco[1], Luca Marciani[2], Snow Stolnik[1], Martin C. Garnett[1]

1, School of Pharmacy, University Park, University of Nottingham, NG7 2RD

2. School of Medicine, QMC, University of Nottingham

Key words

Iron oxide nanoparticles; polymer coating; PEG-copolymer; nanoparticle stability; MRI contrast agents

Abstract

Iron oxide nanoparticles (IONP) have many possible uses including as MRI contrast agents, for drug delivery and cell labelling, but need to be stabilised and to be rendered biocompatible through appropriate coatings. Many current coatings are suboptimal, so we have investigated methodology to produce thin coatings using biocompatible polymers. We have produced uncoated IONP by a co-precipitation method in a range of sizes and subsequently coated the nanoparticles using poly(glycerol adipate) using the interfacial deposition method. To produce the necessary thin coatings a relatively small addition of polymer (approx. 0.1-0.2mg polymer per 38mg IONP) was necessary. A number of different PGA polymer variants with different physicochemical properties were used and the results suggested that the polymer properties also affected the coating process. Optimum coatings only a few nm thick (1-3nm) were obtained with a linear poly(ethylene glycol)-PGA copolymer modified with 40% pendant oleic acid moieties. The resulting sterically stabilised IONP were stable against aggregation at and above physiological salt concentrations. Preliminary experiments demonstrated that the nanoparticles had relaxivity values comparable to commercially available IONP of a similar size and could be taken up readily by cells. This coating method therefore shows promise for a variety of medical applications.

1 Introduction

Iron oxide nanoparticles (IONP) have been proposed for many biomedical uses including as MRI contrast agents, as a potential route to generate hyperthermia for cancer treatment, and for various drug and nucleic acid delivery systems [1] and [2]. IONP have also been proposed as marking and tracking moieties for cells [3] and [4]. For these different applications, a variety of nanoparticle sizes have been used. Various physical and chemical synthesis methods can produce small nanoparticles with an average size under 10 nm [5] and [6]. Superparamagnetic IONP of magnetite with a mean diameter of 10 nm and narrow size distribution have been synthesized by the co-precipitation method [7]. Gupta and Curtis [8] have prepared IONP by using the chemical precipitation method and these were found to be small in size, around 13.6 nm measured by transmission electron microscopy (TEM). The important parameters that affect size of IONP during synthesis are the reaction conditions such as pH value, temperature, stirring rate and dropping speed of each solution [9] and [10] which allow control over the IONP sizes produced.

A significant factor to overcome in the development of IONPs for these applications is the tendency of metal nanoparticles to aggregate because of attractive van der Waals or magnetic dipole-dipole interactions, and due to the attraction due to magnetic forces [11]. Stability can be achieved by one of two fundamental mechanisms: either the presence of an electrical double layer on the particles or the presence of a polymer providing steric stabilisation [12]. In order to prevent particle aggregation, a steric or electrostatic repulsion can be produced by coating the particles with polymers. This property of the surface coating is important in both MRI and drug delivery applications.

For MRI studies, coatings using dextran or carboxy dextran have typically been employed in the commercially available formulations. While these have the advantage of water solubility leading to a simple coating method by adsorption, these polymers tend to produce quite thick

coating layers which are readily desorbed. The choice of a hydrophilic polymer like dextran may also tend to make the particles more biocompatible by reducing opsonisation, but is not particularly effective at this function compared to polymers like poly(ethylene glycol) (PEG) [13]. Biocompatible and hydrolytically degradable polymers such as poly(D,L,lactide-co-glycolide), poly(D,L-lactide), and poly(glycolide) [14, 15] and [16] have also been reported as coating materials. However, coating methods here tend to encapsulate the IONP into larger polymer nanoparticles or to form very thick particle coatings.

We wished to explore methodology to produce much thinner coatings which would have advantage in drug delivery in increasing relative payloads and using a more effective polymer for controlling biodistribution.

Over the last decade we have used a different polymer, poly(glycerol-adipate) (PGA) in our nanoparticle drug delivery work. It is an enzymically biodegradable polymer made from non-toxic monomers [17]. It has the capability to self–assemble into small particles and has showed the ability to entrap an anticancer drug with a high efficiency [18]. These characteristics suggest that PGA polymers are useful for preparing nanoparticles for drug delivery. PGA has a pendant hydroxyl group that can be modified with a range of different substituents [19], [20] and [21].

In this study, we have used both unmodified PGA and PGA where the pendant hydroxyl groups have been modified with medium and long chain fatty acids (PGA C_8 and PGA40%C_{18}) to produce more hydrophobic polymers. Polyethylene glycol (PEG) is often used to form copolymers with hydrophobic polymers to produce micelles and nanoparticles with improved surface properties. Two PEGylated versions of PGA have also been investigated, a PEGylated succinic acid modified PGA (PEG-PGA-SA) which also provides additional carboxyl groups similarly to carboxy dextran, and also the more hydrophobic PEGylated PGA40%C18 (PEG-PGA40%C_{18}). In this study, a co-precipitation method was used to synthesise iron oxide

nanoparticles over a range of sizes with potential for a variety of uses as outlined above and coated using a simple method we have developed here. The characteristics and physiological stability of these particles are described together with some preliminary example uses of these polymer coated nanoparticles.

2 Materials and Methods

2.1 Materials

Poly(Glycerol Adipate) with an estimated MW of 10KDa and its 40% C_{18} derivative (PGA40%C_{18}) were prepared as previously described [22] (see Figure 2 for structures).

Polymers Used in This Study

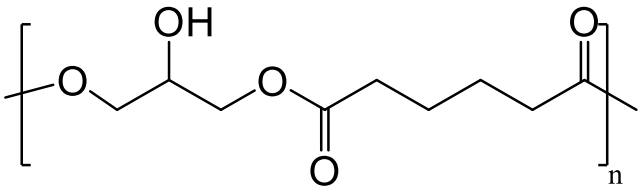

A. Structure of Poly (glycerol adipate) backbone

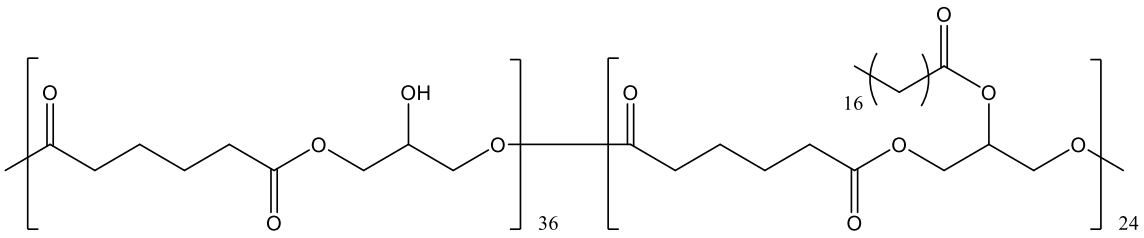

B. Structure of Acylated poly(Glycerol Adipate) (40%C_{18})

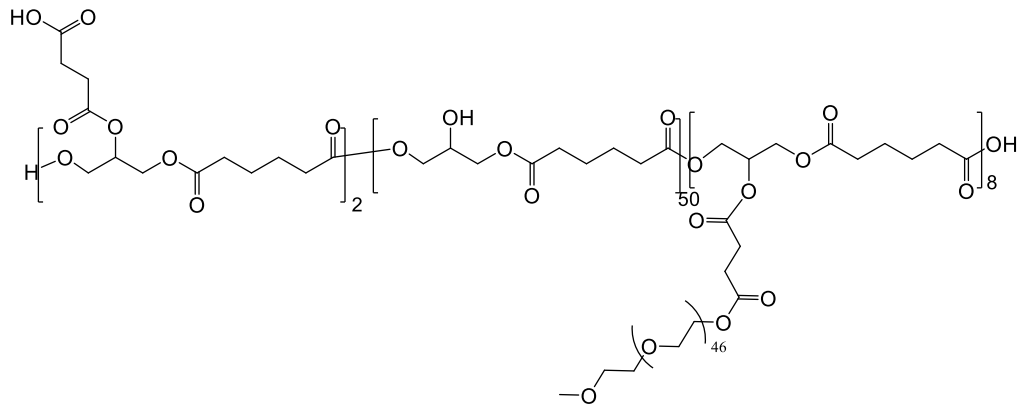

C. Structure of PEG-PGA-SA which has Pendant PEG chains from reaction with pendant succinic acid side chains on succinylated PGA.

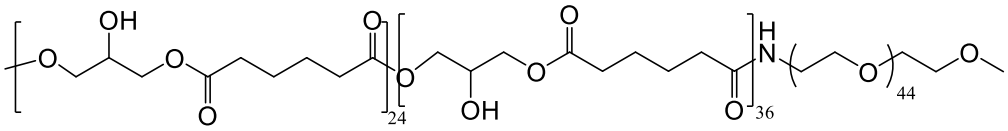

D. Structure of poly(Ethylene Glycol) poly(Glycerol Adipate) 40%C_{18}.

Figure 1. Structures of PGA and Modified PGA polymers used in this study. A. PGA, B. Acylated PGA (PGA40%C_{18} and PGA40%C_8), C. PEG-PGA-SA and D. PEG-PGA40%C_{18}

2.2 Methods

2.2.1 Synthesis Processes

2.2.1.1 Synthesis of PGA

PGA was synthesized by enzymatic (Novozyme 435) reaction of divinyladipate (DVA) and glycerol in anhydrous tetrahydrofuran (THF) for 24 h as described previously [23]**.** By keeping both a strictly equimolar stoichiometry ratio of the two monomers, constant mechanical stirring

and by controlling the reaction temperature below 50°C a reproducible polymer with Mn of around 13,000 Da and D of circa 2.3 can be easily obtained.

2.2.1.2 Synthesis of Acylated PGA (PGA40%C_{18} and PGA 40%C_8)

PGA substituted with 40% C_{18} acyl groups has been previously described [22]. Briefly, dry THF (20 ml) was added to PGA (2 g, 0.16 mmol) in a round bottomed flask and refluxed under a nitrogen atmosphere at 80 °C to dissolve the polymer. Stearoyl chloride (656 mg, 43 mmol) in dried THF (0.5 ml) was then added to a flask containing the PGA and pyridine (0.5 ml) was also added to the mixture. The system was refluxed for two hours, dissolved in 30 ml of dichloromethane (DCM) and then washed three times using water (20 ml) with 1 M HCl (0.5 ml) followed by two washes with water alone (40 ml) following by drying using $MgSO_4$. Product was obtained by removal of DCM using a rotary evaporator.

2.2.1.3 Synthesis of PEG-PGA 40% C_{18}

Briefly, PEG-NH_2 with M_n of 2000 was dried by $MgSO_4$ in DCM and precipitated with cold ether, then filtered and dried under vacuum. Carbonyl di-imidazole (CDI) was prepared by dissolving CDI (40 mg, 0.25 mmol) in DCM (5 ml). The PEGylation reaction was carried out by dissolving PEG-NH_2 (110 mg, 0.05 mmol) in chloroform (3 ml) in a double-necked round–bottomed flask and then CDI (1 ml) solution was transferred to the CH_3-O-PEG-NH_2. The polymer PGA 40%C_{18} (600 mg, 0.05 mmol) was then dissolved in DCM (10 ml) under stirring. The CH3-O-PEG-NH_2 solution was added to the PGA40%C_{18} solution. The resulting product was stirred for 7 days under a nitrogen atmosphere. After this time, the product was obtained by removal the solvent by vacuum. Excess unreacted polymers PEG or PGA were also removed by washing the product by diethyl ether (1.5 ml) three times. The product was then allowed to dry for 30 min.

PEG-Poly(Glycerol Adipate)-succinic acid (PEG-PGA-SA) was synthesised starting from PGA. Using an estimated 60 repeat units along the main backbone, succinylation was performed in THF using 10% mol/mol of Succinic anhydride compared to PGA units. The reaction was almost quantitative. Subsequently, PGA was added drop-wise to a DCM/THF solution of monomethylated PEG (mPEG), dicyclohexyl carbodiimide (DCC) and Dimethyl amino pyridine (DMAP) equimolar with the succinyl groups. The crosslinked precipitate was removed by filtration and the soluble polymer precipitated in cold Hexane. PEGylation was around 80% in yield, giving an estimated small excess of succinic acid pendant groups.

2.2.1.4 Preparation of iron oxide nanoparticles (IONPs)

Method 1

IONPs were prepared by alkaline co-precipitation using a modified method based on that by Kresse et al [24]. Ferrous chloride.$4H_2O$ (0.49 g) was suspended in ferric chloride .$6H_2O$ (1M, 5.06 ml ferric-to-ferrous 2.06:1 molar ratio. Ultrapure water (6 ml) was added under nitrogen with rapid stirring then heated to 80 $^{\circ}$C for 1hr. The mixture was cooled to room temperature then precipitated by adding NaOH (6 M, 6.5 ml) rapidly. After adding 4 M HCl to the mixture to acidify to pH 0.5, it was refluxed for 1 hr under nitrogen gas. In this step, the black colour turned brown. The reaction was allowed to cool to room temperature; the mixture was dialyzed using dialysis tubing with a molecular weight cutoff (MWCO) of 1000Da overnight against deoxygenated water to remove any salts.

Method 2

This second method also used the modified co-precipitation method but with a different ferrous to Ferric ratio and with control of the pH in the second step.

Ferrous chloride.4H_2O (0.98 g) was suspended in ferric chloride .6H_2O (1.036M, 4 ml ferric-to-ferrous 0.84:1 molar ratio). Pure water (10 ml) was added under nitrogen with rapid stirring then heated to 80 $^{\circ}$C for 1hr. The mixture was cooled to room temperature then precipitated by adding different amounts of NaOH (6 M) rapidly. The final pH of the mixture was controlled by adding 4 M HCl, then the temperature was elevated to 100°C and refluxed under nitrogen gas for 1 hour followed by cooling. In this step, the black colour turned brown. The reaction was allowed to cool to room temperature; the mixture was dialyzed using a MWCO 1000 dialysis tubing overnight against deoxygenated water to remove any salts.

2.2.1.5 Preparation of polymer coated IONPs

Method 1

Coating of pre-prepared iron oxide nanoparticles was carried out using a method based on the interfacial deposition method for nanoparticle formation described by Fessi et al (1989) for polymer nanoparticle production [25].

The required amounts of the polymers were weighed accurately in order to make stock solutions in acetone (20 mg in 2 ml). Varying amounts of polymers (equivalent to 0.05 mg, 0.1 mg, 0.2 mg and 0.3 mg) were taken from these stock solutions and diluted to make them up to 2 ml with acetone. Different amounts (0.1-1.0mg) of PEG-PGA 40% C_{18} (0.2 mg of polymer in 2 ml acetone) were added dropwise to an aqueous solution containing IONPs (2 ml) as prepared above diluted with water (3 ml) under gentle stirring. The product was stirred overnight in a fume hood to allow evaporation of the organic solvent.

Method 2

This method uses a similar principle and similar amounts of materials to method 1, however method 2 is a continuous method rather than a batch method. Four polymers PGA 40%C_8, PGA 40%C_{18}, PEG-PGA-SA and PEGylated PGA 40%C_{18} were used for coating the IONPs using this method.

The IONP solution (2 ml nanoparticles and 3 ml of DI water) and polymer solution (2 ml) were mixed using two pumps and a mixer (Pharmacia LKB, Pump P-1, Amersham Biosciences), with both solutions being pumped at different rates through a mixing chamber in proportion to the volumes of each component. The flow rates were chosen in order to give complete mixing of the reagents over 1–2 minutes. Following mixing, the particle suspension was left on a stirrer overnight in a fume hood in order to completely evaporate the acetone. The coated nanoparticles were collected the next day and further characterised. This modified method was also based on that of Fessi et al. (1989)

2.2.2 Characterization Processes

2.2.2.1 Measurement of Particle Size

Measurement of particle size was carried out using dynamic light scattering on a Viscotek 802 instrument. Results were analysed by intensity distribution. Measurements of the samples were performed using a scattering angle of 90° to the incident beam at 25°C ± 0.1°C. The analysis mode was CONTIN and 10 readings were taken for each sample. The concentration of coated and uncoated IONPs was set at 50 µg/ml for all measurements in order to reach a count of below 300–600 KCps while measuring the samples. The solution was diluted to the desired concentration in DI water and filtered with a 0.2 µm filter and vortexed for 1 minute to remove any aggregates before each measurement. DLS scattering data were collected at room temperature, and processed using Omnisize 3 software. The experiments were repeated three times, and the results of value ± standard deviation were averaged.

2.2.2.2 Zeta Potential Analysis

The ζ-potential of the nanoparticles was determined by laser doppler anemometry using a Malvern Zetasizer. Measurements were performed at 20 °C, on samples appropriately suspended in water.

The nanoparticle suspension (200 µl) was diluted with filtered PBS diluted 1 in 10 (0.5 ml, 15 mM, pH 7.4), and the results were expressed as the mean ± standard deviation for six readings and data plotted in GraphPad Prism. All measurements were carried out at 20°C.

2.2.2.3 Colloidal Stability of IONPs

The colloidal stability of coated IONPs in different environments is very important therefore, the stability of uncoated and coated IONPs was investigated by turbidity measurements using a TECAN Spark 10M plate reader. To the diluted dispersion of IONPs (50 µl), various concentrations of sodium chloride (200 µl) were added to give final concentrations from 1 to 480 mM. Then, vortexing for 5 seconds, and optical density determined immediately at 562 nm (a filter with a convenient long wavelength for measuring turbidity due to colloidal precipitation was used). The experiment was repeated three times to verify the reproducibility, and the average of optical density was calculated.

2.2.2.4 Particle morphology by TEM

The morphology of the particles was examined using TEM (Jeol Jem 1010 electron microscope, Japan) both without staining and with background contrast staining. For the unstained samples, one drop of the sample was placed for 1 minute on the copper grid with a formvar carbon film. The excess of the sample was wicked away with the aid of filter paper. The sample was then ready for analysis by TEM. For the stained samples, the particle

suspension was diluted with 3% w/v phosphotungstic acid at a 1:1 ratio and adjusted to pH 7.5 with potassium hydroxide. One drop of the sample was placed for 1 minute on a copper grid coated with a formvar carbon film. The excess of the sample was wicked away with the aid of filter paper. The sample was then ready for analysis by TEM.

2.2.3 Ferrozine Assay for Measuring iron content of IONPs

Quantitative determination of IONP content in suspension, cell and culture media samples was performed using the ferrozine assay as this assay is an absorbance based assay for determine soluble iron [26]. IONPs (500 µl) were first solubilizing by addition of 12 M HCl (500 µl). This mixture was incubated at room temperature for 1 hour with gentle mixing and then neutralised with 12 M NaOH (500 µl). Ammonium acetate solution (50 µl, 10 M) and 10 mM ferrozine (300 µl) were added to each sample. At the end of reaction, 200 µl of each sample was placed into the 96-well plate. Absorbance was measured at 562 nm using Multifunction Plate Reader, TECAN Spark 10M. Determination the amount of IONPs was based on a standard curve prepared using known concentration IONPs in a way similar to that of the sample.

2.2.4 Relaxivity Measurement

Relaxivity is a measure of the ability of a MRI contrast agent to increase the relaxation of the surrounding hydrogen protons that can then be used to enhance contrast in MR images. For the relaxivity measurements, aqueous suspensions of various IONP concentrations were prepared in water. IONP suspensions with sizes 22, 50 and 80 nm, with varying concentrations of 0.01, to 1.79 mmol/L were used. The T1 and T2 relaxation times of hydrogen protons in the aqueous suspension of the IONPs were measured at room temperature using a 1.5T Philips Achieva

MRI scanner (Philips Healthcare, Best, Netherlands). The specific relaxivities were calculated according to:

$$1/\Delta T1 = r1.\,[C] \quad \text{and} \quad 1/\Delta T2 = r2.\,[C]$$

Since ΔT1 and ΔT1 are relaxation rate in seconds, [C] is the concentration of contrast agent and r1 and r2 represent relaxivity. The relaxation rates of a contrast agent in a solution are obtained by plotting changes in relaxation rates (1/T1) and (1/T2) at different concentrations.

2.2.5 Cell studies

2.2.5.1 Preparation of the nanoparticles for cell work

To avoid hypotonicity, nanoparticles in water (5 ml) were added to a concentrated medium to give a stock particle solution. Particles were then diluted in a normal cell culture medium to give various concentrations of the nanoparticles. Then the particles were added to the cells. The coated IONPs were calculated to be at concentration of 0.07 M (3.92 mg/ml)

2.2.5.2 C6 cells

The C6 cell line was obtained from the American tissue culture collection and is a brain derived rat glioma line which has fibroblast morphology and adherent growth properties. It was routinely grown in full culture media supplemented with 10% foetal calf serum. 10x Minimum Essential Medium (MEM) (10 ml) was added to new-born calf serum (10 ml) and then sodium bicarbonate (5 ml) was added to the mixture followed by the addition of glutamine (ml 200 mM glutamine). The medium was then made up to 100 ml with purified water and filtered through a 0.2 µm sterile filter. The C6 glioma tumour cells were cultured as monolayer in 75-cm^2 culture flask in medium. Cells were incubated at 37˚C with 5% CO_2 and 100% humidity and passaged every 5-7 days at about 80%-90% subconfluence.

2.2.5.3 Qualitative Nanoparticle uptake by cells

Cellular uptake studies were carried out with PEG-PGA40%C_{18} coated IONPs. C6 cells growing in monolayers on poly(D-lysine)-coated coverslips in 24 well plates were incubated with a quantity of RBITC labelled polymer coated IONPs for 2h and then washed twice with PBS and fixed with 4% paraformaldehyde. The cells were washed again with PBS, medium was removed and then cells were mounted with a drop of DAPI before imaging with fluorescence microscopy. The uptake was evaluated with various volumes of IONP suspension (1 ml, 0.5 ml, 0.2 ml and 0.1ml) prepared as above.

3 Results

3.1 Synthesis of IONP

IONP prepared using the co-precipitation method in the absence of stabilising agents (method 1) were analysed using TEM and DLS, (Fig.2). It is immediately obvious that these uncoated nanoparticles are mainly of a very small size with very little aggregation. Transmission electronic microscopy (TEM) was used to analyse the morphology of the IONP. Different batches showed the same mean particle size calculated by TEM when synthesised under the same conditions. Samples were estimated to be 13.9 ± 3 nm in diameter when stained (Fig.2A) and 13.1 ± 9 nm unstained (data not shown) and showed that the particles were a spherical shape and smooth with a narrow size distribution. The image shows a few larger particles or aggregates, but indicates that the majority of nanoparticles are small. The particle sizes of the intensity distribution from DLS in the figure given below ranged between 6–13 nm as shown in the DLS results in (Fig. 2B). This also shows a good size distribution with few aggregates present.

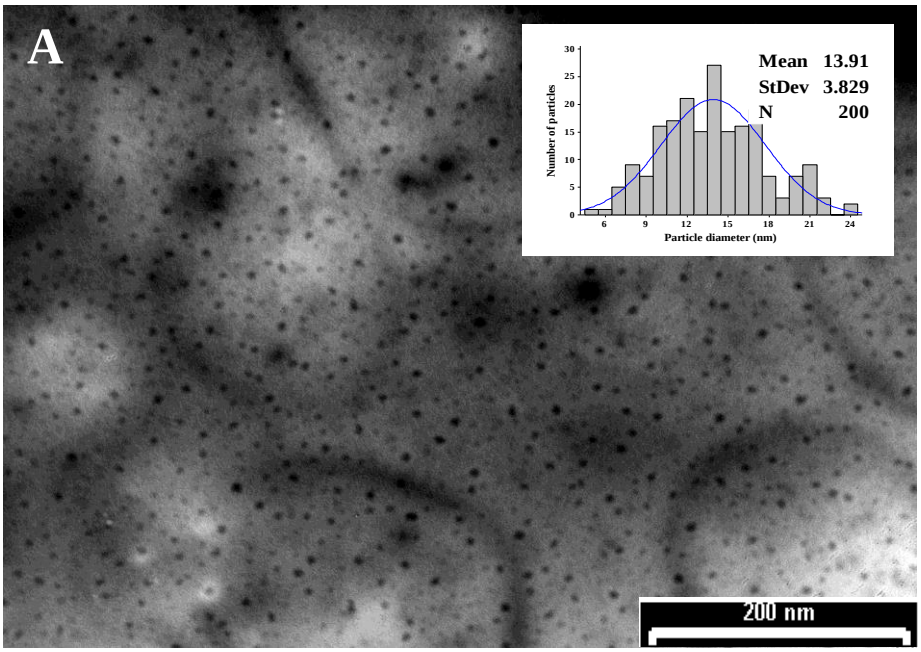

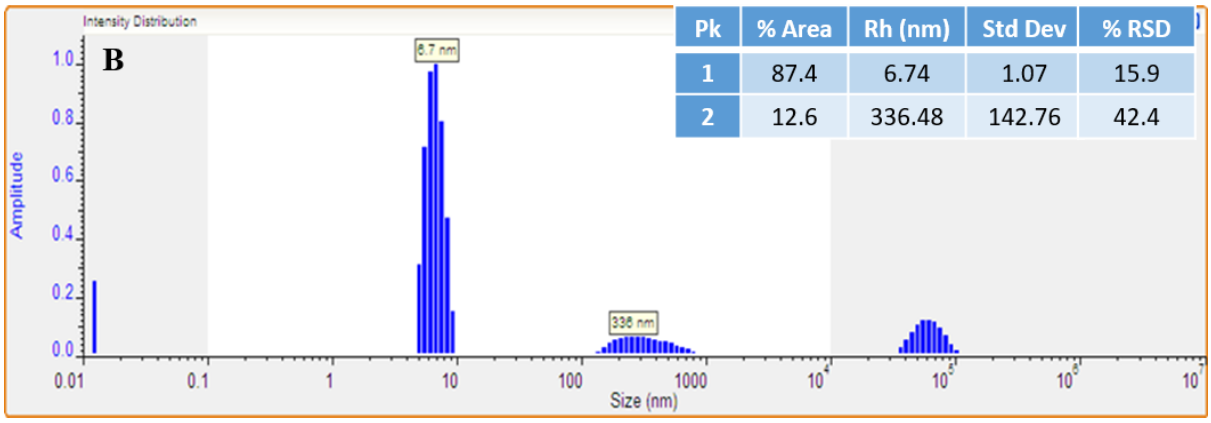

Figure 2: The particle size distribution of IONPs prepared by method 1. A TEM. Particles were prepared by co-precipitation and placed on copper grids, stained with 3% phosphotungstic acid for 2 minutes, and dried (Average size 13.9 ± 3 nm). B Hydrodynamic radii and distribution of IONP by DLS by intensity.

Further methodology to investigate a range of sizes was also developed (method 2) using a range of different pH during the precipitation step of the synthesis. The variation in nanoparticle size as a function of pH is shown in Figure 3 showing that for the smaller sizes a very good control of size was obtained with change of pH, but as the pH was raised above 4 IONP size increased quite markedly together with a greater variation in nanoparticle size. We chose to use nanoparticles of approximately 10, 18 and 25 nm in radius as our standard sizes in this second part of the work, and the DLS characterisation of these particles is shown in Figure 4. It can be seen that all of these preparations resulted in a clean single main peak of IONPs with a narrow size distribution and only a small amount of aggregates.

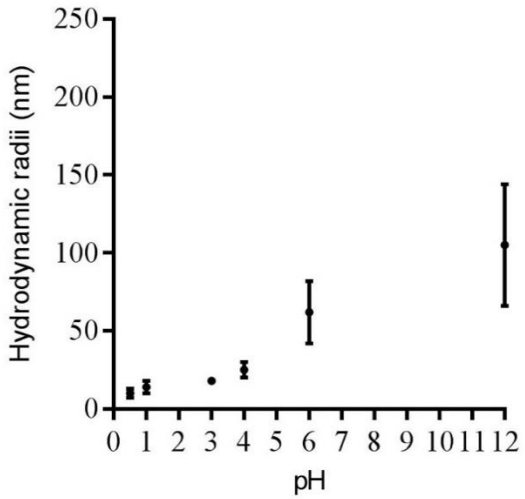

Figure 3: Variation in IONP hydrodynamic radii as a function of pH during the synthesis process. Different sized nanoparticles were obtained simply by varying the sodium hydroxide amount and with variation in the pH of precipitates. The particle size of the nanoparticles was determined by DLS. IONPs produced over the pH range 0.5-4 were of smaller size, as compared to those formed over the pH range 6 and 12, which were larger and with less control over particle size.

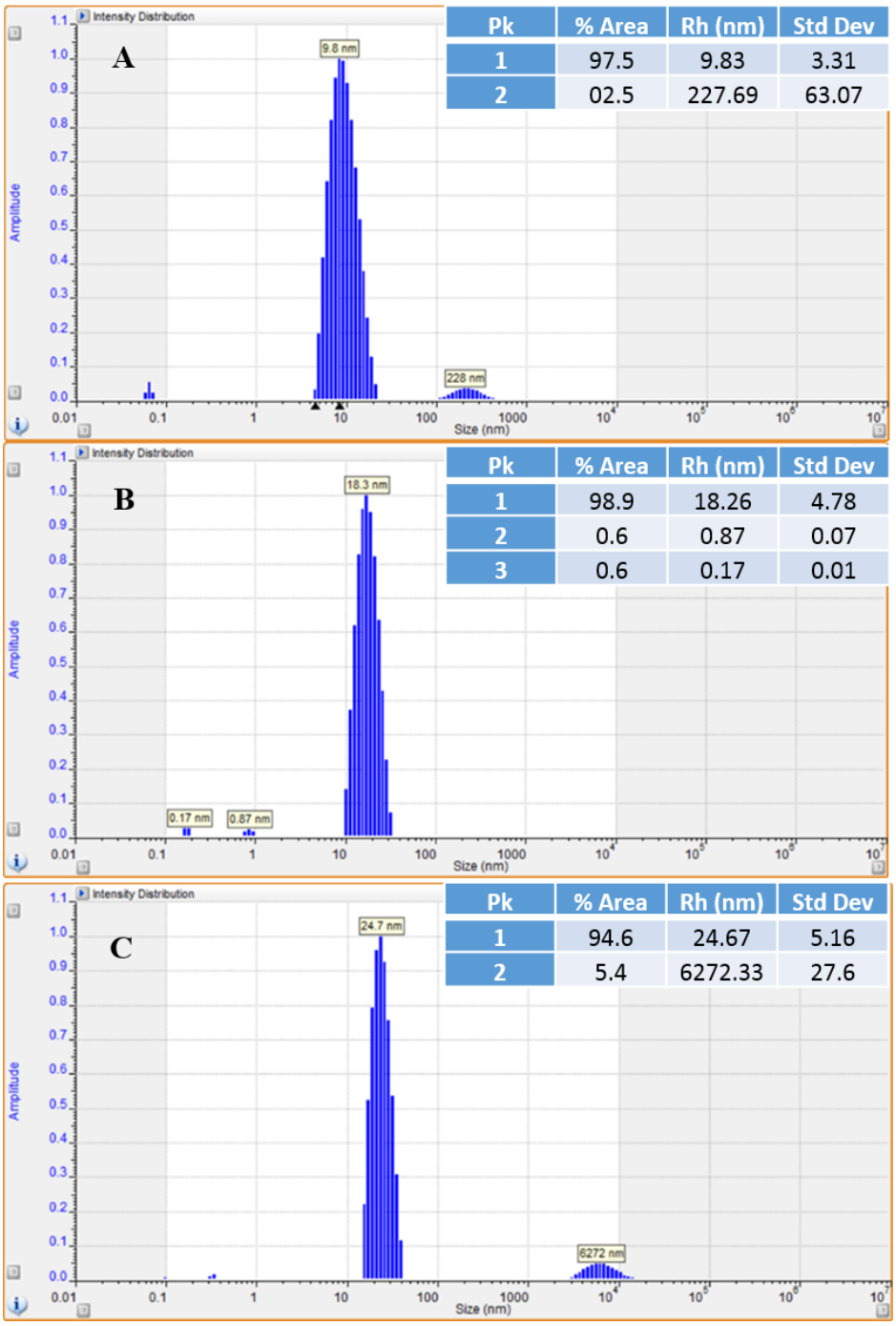

Figure 4: The hydrodynamic radii (Rh) of uncoated IONPs of different size (method 2) by DLS intensity. NPs were prepared by the co-precipitation method at different pH where (A) at pH 0.5, (B) at pH 3 and (C) at pH 4. NP suspension was diluted with ultrapure water to an appropriate concentration to give 300-600 kcps. The Rh of each sample is expressed as the mean particle hydrodynamic radii ± standard deviation of 10 readings.

3.2 Coating IONPs

3.2.1 Coating with PGA

The aim of this work was to derive a simple and convenient method to produce a thin polymer coating on IONP. We chose to use the interfacial deposition method as used for preparing polymer nanoparticles based on other similar work reported in the literature. Using the amounts of polymer in these methods resulted in a range of large and diverse nanoparticles which suggested that an excess of polymer had been used. From geometrical calculations a much smaller amount of polymer was indicated, so this was investigated using a range of different amounts of polymer in acetone (2 ml) using a standard volume of iron oxide nanoparticle suspension (5 ml) estimated to be 38mg iron content (method 1). The results were assessed by DLS as shown in Figure 5. The size distribution of nanoparticles varied with polymer amount in a complex way to give a range of particle sizes and distributions. The preparation giving the smallest particles was that prepared from 0.2 mg of polymer giving coated nanoparticles of 57 nm in diameter with the minimum amount of unwanted larger nanoparticles. This preparation also showed the best distribution by TEM depicting a large number of smooth, small uniform spherical particles well dispersed in the polymer with most of the small coated particles having a particle size 16 ± 5 nm in diameter (see supplementary data, Figure S1).

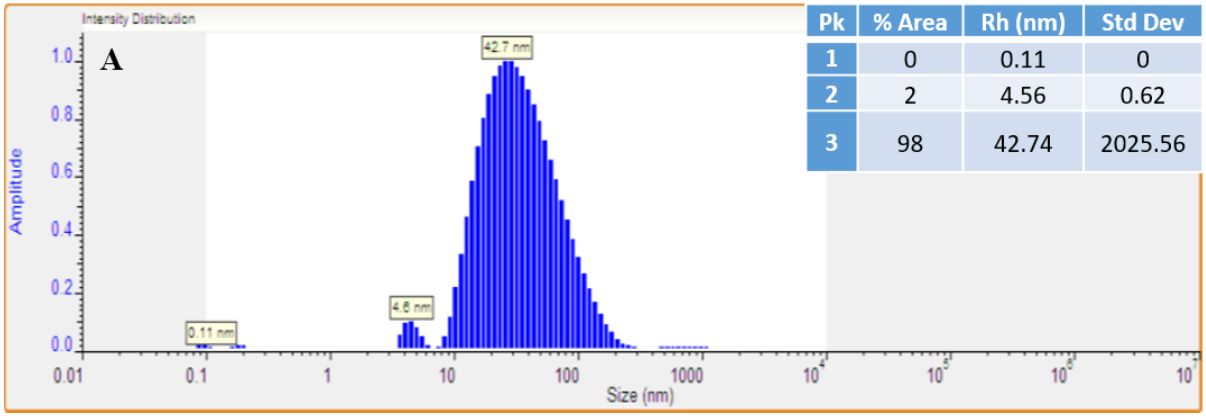

Pk	% Area	Rh (nm)	Std Dev
1	0	0.11	0
2	2	4.56	0.62
3	98	42.74	2025.56

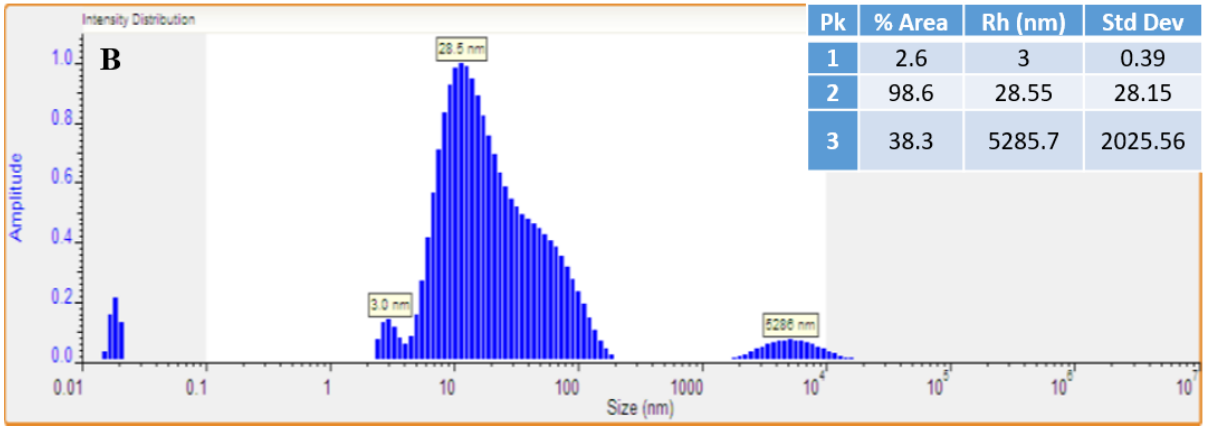

Pk	% Area	Rh (nm)	Std Dev
1	2.6	3	0.39
2	98.6	28.55	28.15
3	38.3	5285.7	2025.56

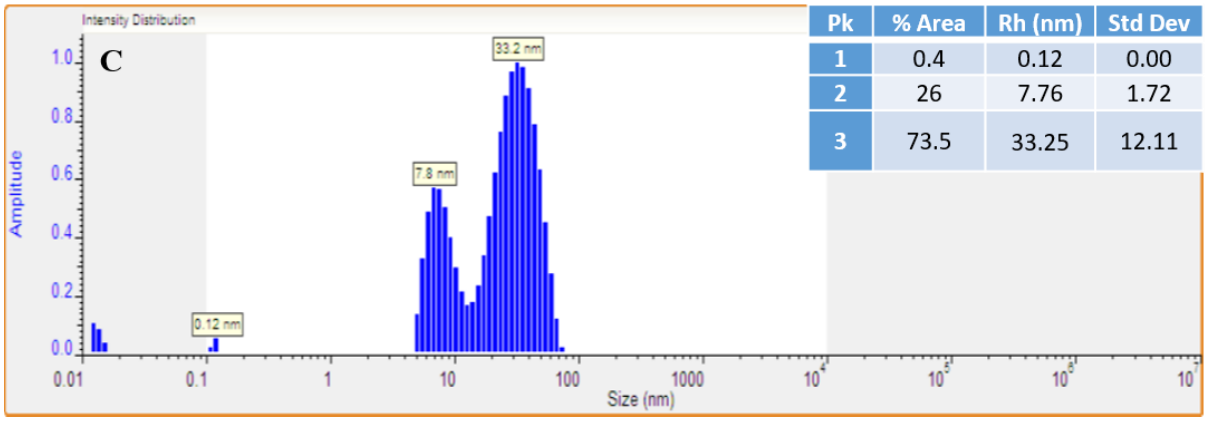

Pk	% Area	Rh (nm)	Std Dev
1	0.4	0.12	0.00
2	26	7.76	1.72
3	73.5	33.25	12.11

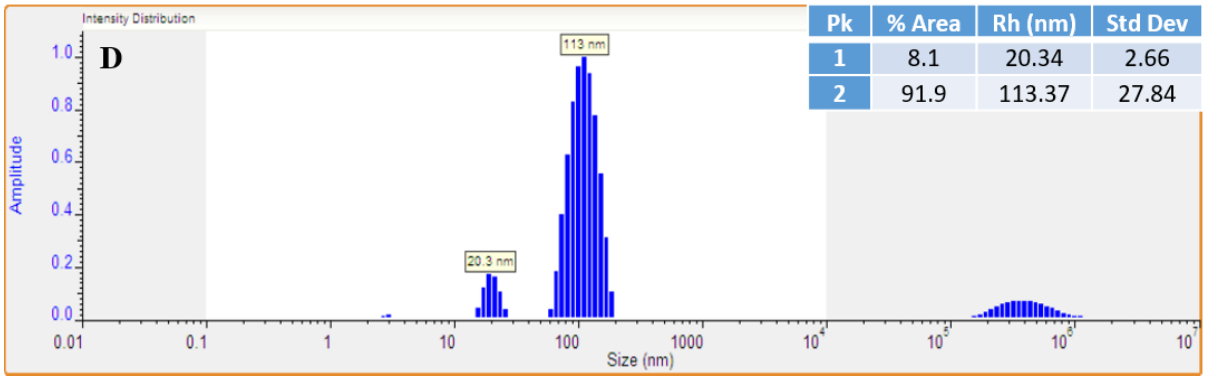

Figure 5. DLS traces showing the size distribution of IONP coated with amounts of PGA. A. 0.1mg, B, 0.2mg, C, 0.5mg, D, 1mg polymer dissolved in 2 ml of acetone.

3.2.2 Exploring modified PGA as a Coating Polymer

Unmodified PGA has a relatively poor efficiency of nanoparticle formation which can be improved by using a modified PGA with pendant acyl side chains to produce a more hydrophobic polymer (Kallinteri, 2005). Different modifications of PGA were therefore explored to investigate the effects of polymer properties on the quality of the coating obtained. The more hydrophobic polymers PGA40%C_8 and PGA40% C_{18} were investigated to look at the effect of increased hydrophobicity while retaining some pendant hydroxyl functionality, and a PEGylated polymer was obtained by reacting succinic anhydride with the PGA and subsequently attaching PEG to the pendant succinyl chains. This latter modification resulted in a more hydrophilic polymer with both carboxyl groups to interact with the iron oxide surface as for carboxy dextran, and PEG for additional stabilisation. To improve the distribution of particles we also adopted a slightly different methodology for the coating procedure, where a flow method was used for the interfacial deposition to maintain the same conditions throughout the polymer addition (method 2).

Table 1. Showing hydrodynamic particle radii of IONP coated with a range of different polymers and polymer amounts.

Coating amount (mg)	Rh (nm)	SD	% area
PGA-40%C_8			
none	18.5	3.31	97.5
0.05	86.36	16.58	90.9
0.1	103.44	22.26	90.4
0.2	111.8	21.92	90.5
0.3	140.96	23.84	93.7
PGA-40% C_{18}			
none	18.5	3.31	97.5
0.05	85.83	18.86	89.5
0.1	91.28	24.08	86.3
0.2	101	19.65	87.7
0.3	120.69	20.19	93.9
PEG-SA-PGA			
none	9.83	3.31	97.5
0.025	140.05	25.35	98.3
0.05	118.7	26.08	89.1
0.1	123.7	22.07	87.4

NPs of hydrodynamic radius 10 nm were coated with different amount of polymer using the interfacial deposition method. NP suspension was diluted with ultrapure water to an appropriate concentration to give 300-600 kcps. Particle size was measured by DLS and was expressed as the mean particle hydrodynamic radius ± standard deviation of 10 readings.

From Table 1 we see that all the additional polymers produced relatively large coated nanoparticles although generally now with a single peak of particles with a relatively narrow size distribution (the DLS distributions of these summarised data can be found in the supplementary information Figures S2, S3 and S4). Of the three polymers, the more hydrophobic PGA40%C_{18} gave the best results, although results for the PGA40%C_8 were very similar. A full DLS trace for all the preparations is presented in the additional data. Although the PEG-SA-PGA did not produce the desired effect of this coating, the use of PEG to give steric stabilisation potentially resulted in a more homogeneous population of polymer coated nanoparticles. PEGylated PGA40%C_{18} (PEG-PGA40%C_{18}) was synthesised for further

coating experiments. These were carried out on the full range of particle sizes prepared. The results of these coating experiments are summarised in Table 2 (the full DLS distributions can be seen in the supplementary information Figures S5, S6 and S7 for 10, 18 and 25nm radius IONP respectively).

The PEGylated hydrophobic polymer produced extremely thin coatings on the smallest IONP which were so thin that the increase in radius representing the coating thickness were less than the standard deviation, so giving little accurate information on the nature of the coating. For the 20 nm radius particles, a slightly thicker layer resulted, about 3 - 5 nm thickness for the best coatings, but again this was of the order of the standard deviation. For the large 25nm radius IONP, the coatings produced were much thicker, 24-45nm.

Table 2. Showing hydrodynamic particle radii of IONP of varying diameters coated with PEG-PGA40%C_{18} over a range of polymer amounts**.**

Coating amount (mg)	Rh (nm)	SD	% area
20nm IONP			
none	9.83	3.31	97.5
0.1	10.07	3.44	98.6
0.2	10.58	3.16	92.3
0.5	10.63	4.48	99.2
40nm IONP			
none	18.26	4.78	98.9
0.1	20.89	5	98.9
0.2	19.93	3.82	99.2
0.5	25.96	6.46	95.1
50nm IONP			
none	24.67	5.16	94.6
0.1	36.84	7.4	81.5
0.2	41.44	8.52	81.1
0.5	45	20	82

NPs of hydrodynamic radius 10 nm were coated with different amounts of polymer using the interfacial deposition method. NP suspension was diluted with ultrapure water to an appropriate concentration to give 300-600 kcps. Particle size was the mean hydrodynamic radius and measured by DLS. The particle size of each sample is expressed as the mean particle hydrodynamic radius ± standard deviation of 10 readings.

In terms of the optimum amount of polymer needed, this was clearly 0.2mg for the medium size where the minimum thickness, smallest standard deviation, and the maximum amount of IONP in the optimum distribution. For the largest IONP, the optimum tried was the 0.1mg amount. For the smallest IONP, the optimum level was not obvious with all coating amounts having different optimum indicators, but all appeared to give useful thin coatings. TEM images of the 10nm radius IONP coated with PEG-PGA40%C_{18} can be seen in Figure 6 which shows also the ovoid nature of particles made by method 2.

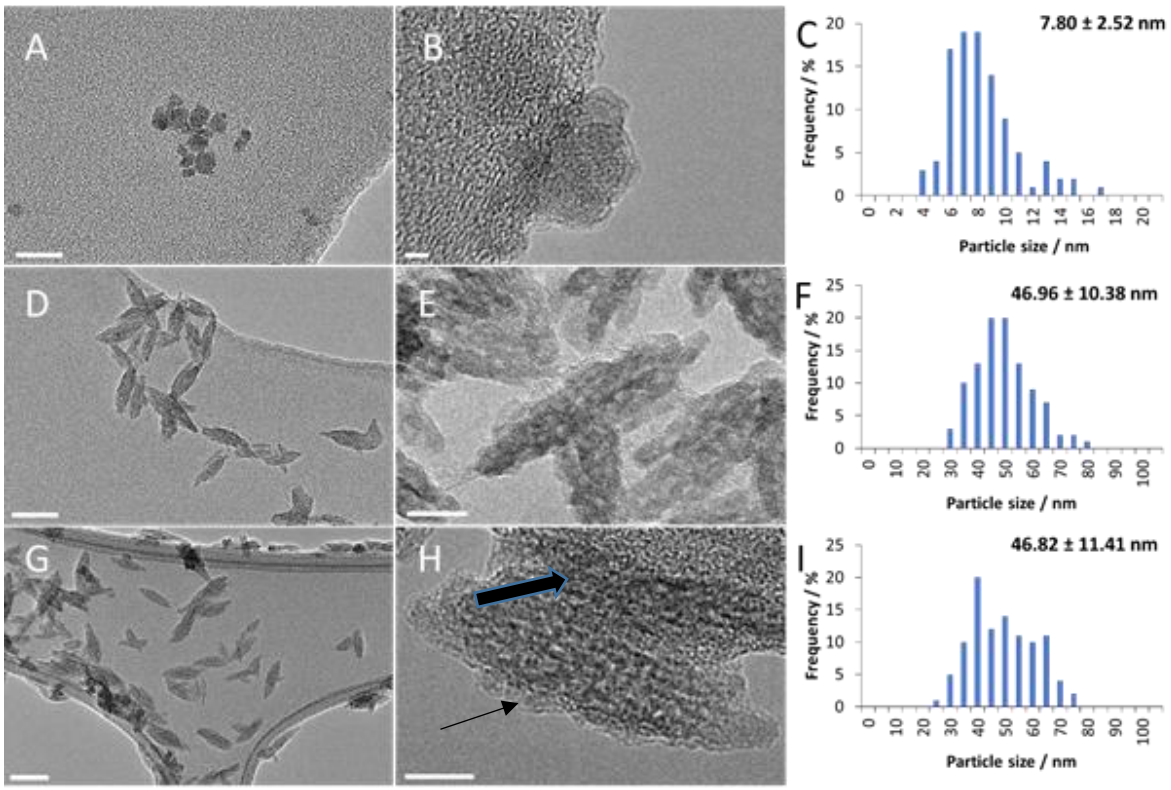

Figure 6: TEM images (A, D, G) and particle size distribution graphs (C, F and I) of different batches of PEGylated PGA 40% C_{18} coated IONPs (10nm radius IONP) where (A and C) 0.3 mg, (D and F) 0.2 mg and (G and I)) 0.1 mg PEGylated PGA 40% C_{18} coated IONPs. Particle size and standard deviation values are inset (N = 100). Higher magnification of each formulation of PEGylated PGA 40% C_{18} coated IONPs, shows visible lattice planes of individual IONPs (darker structured area ,bold arrow) embedded in a polymer matrix (lighter more granular appearance ,light arrow) (B, E and H). Scale bars are (A) 20 nm, (B) 2 nm (D and G) 50 nm and (E and H) 10 nm.

3.3 IONP stability

The IONP were assessed by laser doppler anemometry to assess the change in charge following coating with PEG-PGA40%C_{18} (Figure 7). All IONP initially had a positive zeta potential at about 40mv which changed to a negative zeta potential of about 35-40 mv on coating with polymer. There was a trend towards a less negative zeta potential with increasing amount of polymer on the 20nm diameter IONP but the changes were not statistically significant.

The stability of the particles was explored further by addition of salt to assess the particle stability under physiological conditions. (Figure 8). Optical density of the uncoated IONP suspensions substantially increased on addition of even a small amount of salt demonstrating the easy aggregation and poor colloidal stability of these preparations. In contrast the coated IONP showed an initial small increase in optical density and then plateaued giving no further increase up to the maximum salt concentration tested at 480mM. This suggested a small population of unstable IONP but the majority being stable to salt concentrations well above physiological levels

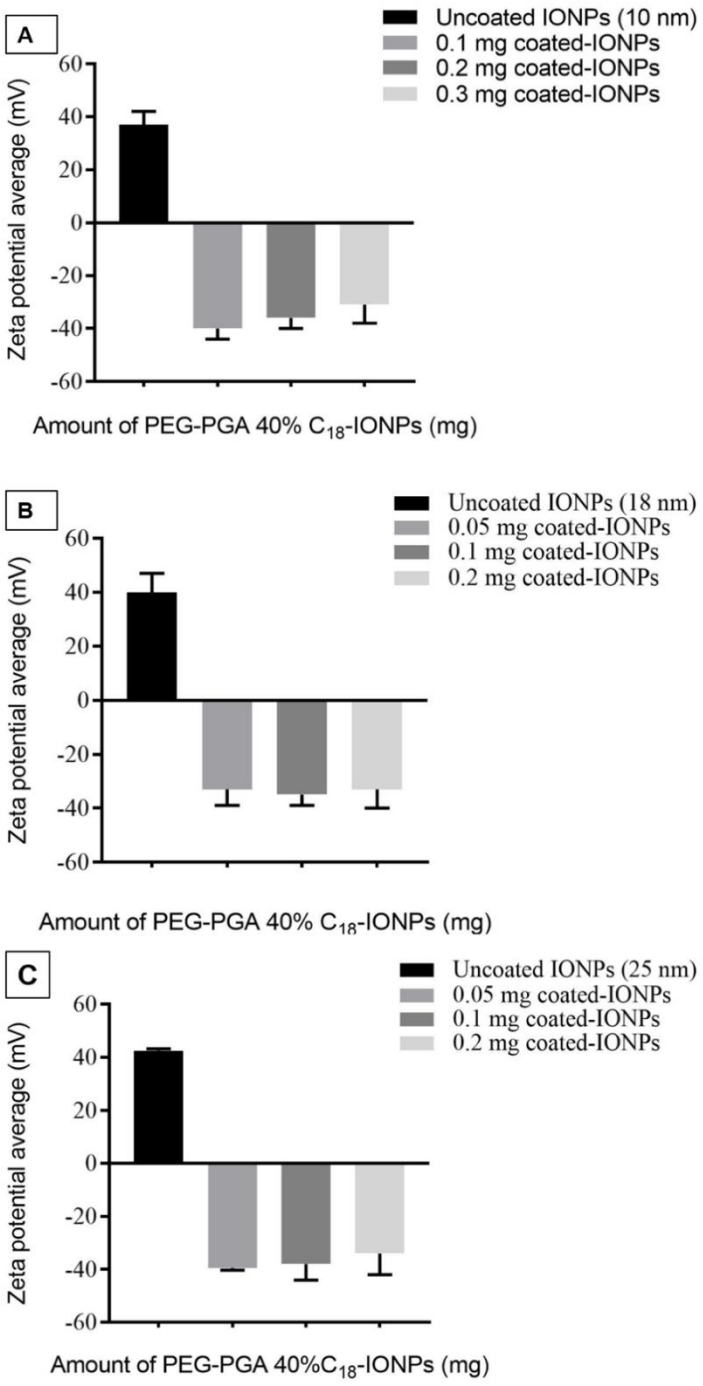

Figure 7: Surface charge of uncoated and PEGylated PGA 40% C_{18} coated IONPs where, (A) zeta potential of Rh 10 nm, (B) zeta potential of Rh 18 nm and (C) zeta potential of the biggest Rh (25 nm) of uncoated and coated with PEGylated PGA 40% C_{18} of different amounts. The zeta potential of all formulations was not significantly decreased when the amount of PEGylated PGA 40% C_{18} was increased. Zeta potential measurements were performed in PBS (15 mM) at pH 7.4 using Zeta sizer (Malvern Instruments, Malvern,UK). Results are expressed as the mean ±standard deviation of 5 readings.

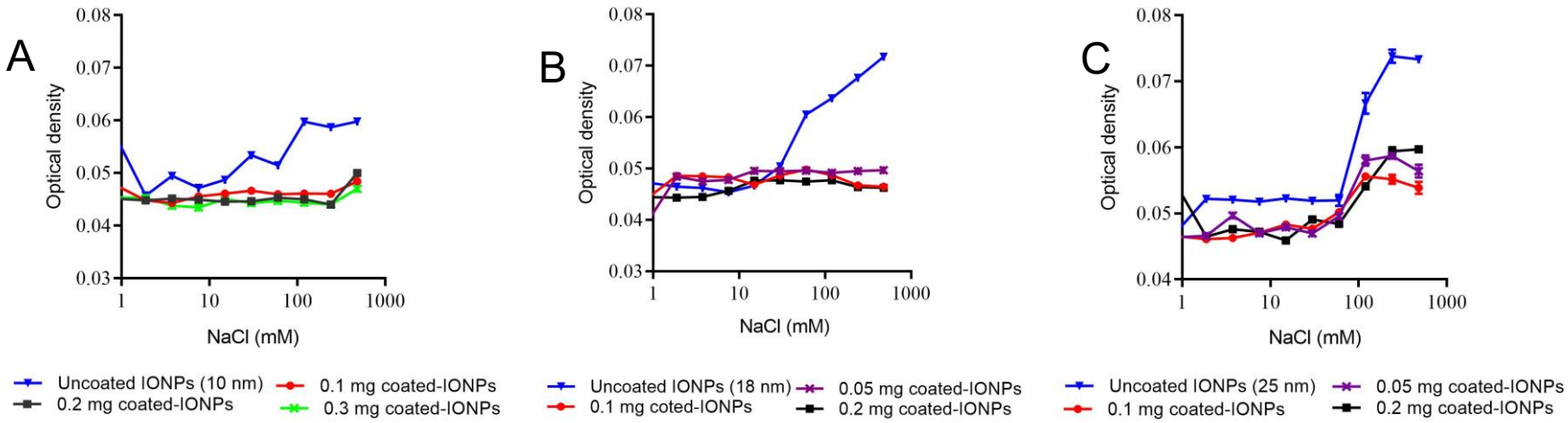

Figure 8: Stabilities of different formulations of uncoated and coated IONPs with different amount of PEGylated PGA 40% C_{18} (0.05, 0.1, 0.2 and 0.3 mg), where (A, B and C) stability of PEGylated PGA 40% C_{18} IONPs resulting from coating IONPs of hydrodynamic sizes 10, 18 and 25 nm respectively. Coated and uncoated IONPs (25 µg/ml) were mixed with different concentrations of NaCl. The absorbance was measured at 562 nm using a TECAN plate reader. For the IONPs absorbance at 562 nm, a significant difference was found between the uncoated and PEGylated PGA 40%C_{18} of different sizes ($P < 0.0038$), however, according to multiple-way ANOVA test, there were no significant differences between 0.05, 0.1, 0.2 and 0.3 mg PEG-PGA coated IONPs ($P>0.05$).

3.4 MRI relaxivity of PGA coated IONPs

Relaxivity measurements of different size polymer coated IONPs were performed in order to assess the effect of the size and the coating thickness on the magnetic properties of IONPs. The trends of 1/T1 and 1/T2 of IONPs were plotted as a function of the iron concentrations as determined by ferrozine assay (See supplementary information Figures S8 for these plots) and the longitudinal and transverse relaxivities (r1 and r2) were obtained by calculating the slope of the above graphs. Both 1/T1 and 1/T2 relaxation rates were linearly proportional to the iron concentration and are presented in Table 3.

Table 3: Results of MRI studies showing r1 and r2 values of polymer coated IONPs obtained at 1.5T compared with commercially available contrast agents.

Coated IONP description	Structure/ particle size (nm)	T1 Relaxivity (L/mmol-s)	T2 Relaxivity (L/mmol-s)
Novel polymer coated IONP	PEG-PGA40%C_{18} /22nm	0.75	6.06
Novel polymer coated IONP	PEG-PGA40%C_{18} /50nm	4.73	39.15
Novel polymer coated IONP	PEG-PGA40%C_{18}/ 80nm	0.14	0.86
Feruglose NC100150	PEGylated-starch coated IONPs /20nm [27]	20	35
Sinerem®(AMI-277)	Dextran coated IONPs /20-40nm [27]	21.6	44

IONPs of size 50 nm give rise to higher molar relaxivity r2 than 22 and 80 nm. The r2 value is 39.15 mmol-1sec-1 for particle size 50 nm which is similar to the values reported for Feruglose NC100150 and Sinerem® (AMI-227) also included in Table 3. A low r2 value was not expected for particle size 22 nm which may attributed to very low concentration of iron used compared to the other formulations. Polymer coated IONPs of size 80 nm showed the lowest r2 value.

3.5 Uptake of coated IONP

For drug delivery and cell marking studies it is important that cellular uptake of nanoparticles occurs. This was investigated using fluorescently labelled IONPs and C6 rat glioma cells. The particles were labelled with rhodamine B isothiocyanate which has been previously reported to label PGA nanoparticles and to give a stable labelling with negligible loss of label [28]. Cells were then incubated with varying quantities of coated IONPs and the uptake monitored using fluorescence microscopy after 2 hours (Figure 8). A good uptake of IONP was seen across all amounts of particles given with a visually obvious increase in uptake with increasing amounts of IONP added. Uptake was unaffected by the presence or absence of serum in the medium (uptake in absence of serum not shown). A good uptake of IONP was seen across all amounts of particles given with a visually obvious increase in uptake with increasing amounts of IONP added. Uptake was unaffected by the presence or absence of serum in the medium (uptake in absence of serum not shown).

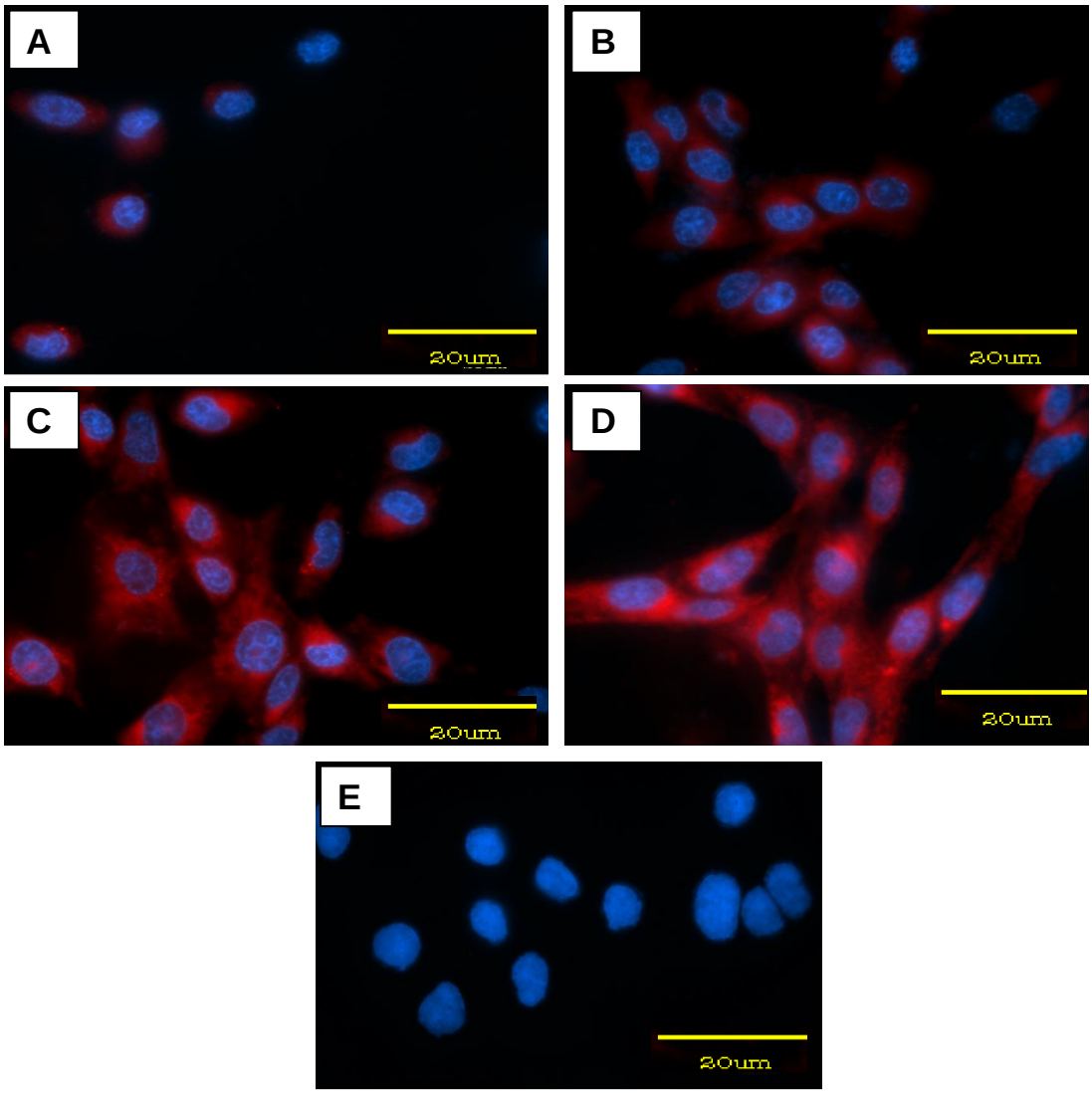

Figure 9: Fluorescence microscopy images of PEG- PGA 40%C_{18}–IONPs incubated with C6 Cells in the presence of serum for 2hr. A, 0.1ml; B, 0.2 ml C, 0.5 ml; D, 1 ml; E, control untreated cells (Scale bar 20 µm).

4 Discussion

To carry out coating without interference from existing stabilisers we chose to synthesise our own IONP rather than purchase commercially available samples. Using the co-precipitation method it was possible to produce small IONP of approximately 13 nm in diameter by both DLS and TEM. This is a size range comprising most of the reported IONP and within a similar

size range to that reported for the most advanced diagnostic IONP contrast agents. Co-precipitation is the simplest, cheapest method which involves the simultaneous precipitation of Fe^{2+} and Fe^{3+} ions in basic aqueous media [29]. Gupta and Curtis [8] have prepared IONP by using the chemical precipitation method and these were found to be small in size, around 13.6 nm measured by TEM. A similar outcome has been achieved with particles made by the Aqueous $FeCl_3$ and $FeCl_2$ solutions are mixed at a concentration ratio of Fe (III)/Fe (II) = 2/1 in an aqueous ammonia solution, yielding Fe_3O_4 NPs with diameters from 3 to 15 nm using the co-precipitation method. This method resulted in suitable IONP unstabilised by any coating which were a single peak of narrow dispersity and which could be used for coating experiments with our polymers.

Previous work on polymer coatings for iron oxide particles can be divided into hydrophilic and hydrophobic polymers. Hydrophilic polymers such as dextran, or carboxy dextran are widely used in clinically approved MRI formulations. They are applied by simple incubation with IONP and produce an adsorbed coating which can desorb [30]. Dextrans also produce surfaces which have poor steric stabilisation [13]. Hydrophobic polymers offer the prospect of polymers which will not desorb so readily and can be produced as co-polymers with PEG. However, coating methodologies are more complex and typically coated particles are reported to be much larger than uncoated particles [31].

To produce IONP with a thin polymer coating with a hydrophobic polymer it was found necessary to have a relatively small amount of polymer present. The smallest most consistent coated nanoparticles using PGA were produced with 0.2 mg of PGA in 2 ml of acetone. Decreasing the amount of PGA still further to 0.1 mg produced larger particles. The general explanation for this phenomenon with change of the polymer amount is quite complex. In the

absence of iron oxide nanoparticles, a high concentration of polymer is necessary for good nanoparticle formation with PGA and all nanoparticles are large, around 100-200nm (Kallinteri 2005). Under these conditions, in the presence of IONPs, these IONPs are just incorporated into the large polymer nanoparticles, and the other parameters have little effect on particle size. There is too much polymer present to form just a small coating of polymer around the iron nanoparticles. Prozerov et al [32] have reported that a large amount of the polymer leads to an increase in the particle size. When the PGA amount came down to low levels (1.0 mg or lower) mixtures of both large polymer nanoparticles and individually coated IONPs were produced. With too little polymer present e.g. 0.1mg, the IONP tended to aggregate and resulted in more, larger aggregates of either aggregated IONP coated with polymer or aggregates of coated IONP.

Although some nice preparations of coated IONP were achieved, single peaks of coated IONP with very small coating layers were not obtained, so a number of measures were taken to improve the methodology and formulation. For most of the remaining work, the nanoparticles were produced by method 2 to give a range of different particle sizes to work with and were also coated using coating method 2. In this second method a continuous rather than batch process was used, but with the same proportions of materials. This method results in more consistent production of particles for a variety of nanoparticle preparations (unpublished results).

Firstly, a range of different modified PGA polymers were used to explore the effect of different physicochemical properties on the coating process. The more hydrophobic acylated polymers were used with the idea that more hydrophobic polymers may produce a better deposition on the IONP nuclei. Of the two polymers used, the 40% C_{18} polymers produced marginally smaller coated IONP than the 40% C_8 polymer. This was probably due to the increased hydrophobicity of the C_{18} side chain compared to C_8. In contrast the hydrophilic PEGylated polymer which

had some additional carboxyl groups so having some similarity with carboxy dextran, produced nanoparticles which were considerably larger. The number of carboxyl groups were relatively small (estimated at 2 groups per polymer chain) and the presence of a number of pendant PEG chains per polymer molecule may have interfered sterically with the adsorption of the polymer chains onto the IONP surfaces. This structural factor may have been responsible for this relatively disappointing outcome with this polymer. The PGA40%C_{18} polymer was therefore taken forward for further studies by synthesis of a PEGylated polymers with a single PEG moiety attached to the terminal carboxyl group of the polymer. Looking at the results from table 3, this was seen to be very effective in providing a good thin coating on a range of different IONP diameters. The effectiveness of this formulation was probably due to a combination of the hydrophobic C_{18} moieties to give a good deposition, plus the remaining pendant hydroxyl moieties to interact with the IONP surface and the steric stabilisation to give single separated nanoparticles.

As there is a significant change in the surface area to volume ratio over this change in particle radius, it was anticipated that different amounts of polymer may be optimal for coatings for different size IONP. While there was some evidence that this may be the case, the optimal amount of polymer wasn't always clear so a definitive answer on this issue was not found.

Using the optimum amount of a well suited polymer the particle sizes appear to be very good in comparison with other polymer-coated particles reported in the literature. A wide range of polymer coated IONP have been reported using various polymers mostly with particle diameters in excess of 150nm. For example, [33] reported IONPs coated with different polyacrylates using the emulsion/polymerisation method. Average coated particle diameters of 160 ±15 nm, 140 ±20 nm, 150 ±30 nm and 155 ± 20 nm were obtained using poly(alkylcyanoacrylate), poly(ethylcyanoacrylate), poly(butylcyanoacrylate), poly(hexycyanoacrylate)and poly(octylcyanoacrylate) respectively.

IONP typically have a positive zeta potential, whereas PGA polymer NP typically have a negative zeta potential of around 35-40mv due to the presence of the terminal carboxyl group of the polymer. Investigation of the zeta potential showed that the uncoated IONP were positively charged as expected, but all amounts of polymer treatment resulted in a typical negative zeta potential confirming the presence of polymer on the IONP surface. These results was particularly important for the very thin coatings measured on the 10nm radius IONP where DLS did not provide confirmation of coating.

While the surface charge can provide some stabilisation through charge repulsion, steric stabilisation by PEG can be far more effective. To assess the stabilising effect of the PEG, and whether this was sufficient for physiological conditions a titration against increasing salt concentrations was performed. With increasing concentrations of NaCl, particles stabilised by charge become more unstable and can aggregate. Similarly, the PEG moieties of the coating become more dehydrated by releasing the water molecules, and the interaction between the layers increasingly leads to flocculation. At the critical flocculation point the PEG chains become dehydrated, chain-chain interactions become attractive and flocculation occurs [34].

Uncoated nanoparticles were unstable even at the very lowest salt concentration, but the PEG-PGA40%C_{18} coated nanoparticles showed a much better stability. There appeared to be a small initial amount of aggregation in all populations of the polymer coated nanoparticles which was most marked for the largest IONP. This probably indicated a small population of IONP which were insufficiently coated. However, there was no further increase in aggregation even up to the highest salt concentrations used (480mM) which is well above physiological salt concentrations. This confirms that polymeric chains on the surface of nanoparticles have a very important role in colloidal stability, especially at a high ionic strength, acting as steric barriers

against aggregation [35]. Similarly Barerra et al [36], have reported that PEG–silane coated IONPs were stable in NaCl concentration from 38 mM to 320 mM with no precipitation.

IONPs have been recognized to hold a great potential in clinical diagnostic applications as magnetic resonance (MR) imaging contrast agents that have the ability to change the proton relaxivity of water. We have produced a series of polymer coated IONP varying in both size and polymer coating thickness which vary in r1 and r2.The changes of r1 and r2 were complex and could be due to either the particle core size or the coating thickness or both.

In our studies, PEG- PGA 40%C_{18} coated nanoparticles of size 50 nm showed the highest value r2 as compared to particle sizes 22 and 80 nm but the coating layer thickness of IONPs of size 22 and 50 nm were very thin compared to NPs of size 80 nm. IONP of size 50 nm showed the highest r2 relaxivity compared to the smallest particles, which have the thinnest coating layer. This higher relaxivity may attributed more to the particle core size rather than the coating thickness. Ahmed et al. [37] considered the particle size dependence of the relaxivity of hydrogen protons in an aqueous suspension of silica coated IONPs and they found that the relaxivity increased linearly with increasing particle size. In their study, they showed that by increasing the size of IONPs with a magnitude of 17% the r1 and r2 increased with the magnitude of 13% and 22%, respectively.

Surface properties can also have effects on MRI contrast efficiency, as the interaction between nanoparticles and water molecules in different environments occur primarily on the surface of the nanoparticles. In our studies, IONPs of size 80 nm showed the lowest r2 value, which could be due to the thickness of polymer, as the increase of coating thickness leads to an increase in the distance between the particle core and the surrounding aqueous solution (water), resulting in a decrease in the relaxivity. Early investigations carried out by Duan et al suggested that hydrophilic surface coating contributes greatly to the resulting MRI contrast effect [38]. Tong

et al modified the core size of IONPs (14 nm) and the thickness of polymer layer polyethylene glycol (PEG) for the maximal r2 relaxivity per particle [39]. They found the r2 relaxivity of SPIO coated with 1000 Da reached a value of 385 $s^{-1}mM^{-1}$ at 7 T, more than 2.5 fold higher than that coated with PEG 5000 Da. Another study indicated that change in the coating thickness influenced the relaxivity more than core size. An increase in 26% in the coating thickness of IONPs of size 8.78 nm resulted in a decrease of 13.64% in r1 and r2. The significance of a thinner coating thickness layer is considered the major factor of the improved relaxivity. Further optimisation of these particles and coatings may well therefore be a useful way forward for developing better IONP contrast agents.

Cell studies

Studies applying PEG-PGA40%C_{18} to rat glioma cells showed a high level of uptake into cells which was concentration dependent. This shows that despite the presence of PEG on the particle surface which can quite often result in a reduction in cellular uptake of nanoparticles, these particles were still readily taken up into cells. This suggests that these polymer coated nanoparticles are therefore potentially suitable for a range of drug delivery or cell marking applications. However, further studies will be needed to explore more specific applications.

5 Conclusions

A new simple methodology for polymer coating iron oxide nanoparticles has been developed based on the interfacial deposition method. The method results in a thin layer of polymer (only a few nm thick) surrounding the nanoparticle. The coating method is dependent on the use of

the addition of small amounts of polymer consistent with the relative volumes of iron oxide nanoparticles core and the thickness of the polymer coating. The method was most successfully demonstrated using a PEG-PGA40%C_{18} polymer which resulted in a single population of particles with a narrow dispersity and the polymer coating provided stability to aggregation in the presence of physiological amounts of salt. Experiments with other polymers suggested that the relative success of the coating may also depend on the physicochemical properties of the polymer. Polymer coated IONP were taken up by cells rapidly and in a concentration dependent manner so have potential uses in drug delivery and cell tracking. The polymer coated IONP were assessed in a 1.5T MRI scanner and showed relaxivity values comparable with similar sized commercially available iron oxide contrast agents. The thin polymer coating with a hydrophilic surface layer may contribute to this property and suggests that further development of these polymer coatings may be useful for further development of contrast agents.

Acknowledgements

We would like to thank Christy Grainger Boultby and Denise Mclean for technical assistance, and Trevor Gray and Rhys Lodge for assistance and advice on TEM. Also to the late Dr Terry Parker for his expertise and supervision in the cell uptake studies.

Funding

Ahmed Abushrida and Ibteisam Elhuni were supported by grants from the Libyan Educational Ministry for their Ph.D studies.

Conflict of interest

There were no conflicts of interest relating to this work.

Supplementary information

S1. TEM image of IONP coated with PGA0% (0.2mg) in acetone (0,2ml)

S2. DLS distribution of IONP (10nm radius) coated with PGA40%C_8

S3. DLS distribution of IONP (10nm radius) coated with PGA40%C_{18}

S4. DLS distribution of IONP (10nm radius) coated with PEG-PGA-SA

S5. DLS distribution of IONP (10nm radius) coated with PEG-PGA40%C_{18}

S6. DLS distribution of IONP (18nm radius) coated with PEG-PGA40%C_{18}

S7. DLS distribution of IONP (25nm radius) coated with PEG-PGA40%C_{18}

S8. TEM of IONP (10 nm radius) coated with PEG-PGA40%C_{18+}

S9 Plot of proton relaxation rates for IONP coated with PEG-PGA40%C_{18}

References

1. Gupta, A.K. and M. Gupta, *Synthesis and surface engineering of iron oxide nanoparticles for biomedical applications.* biomaterials, 2005. **26**(18): p. 3995-4021.

2. Mahmoudi, M., et al., *Superparamagnetic iron oxide nanoparticles (SPIONs): development, surface modification and applications in chemotherapy.* Advanced drug delivery reviews, 2011. **63**(1-2): p. 24-46.

3. Tsai, Z.-T., et al., *In situ preparation of high relaxivity iron oxide nanoparticles by coating with chitosan: A potential MRI contrast agent useful for cell tracking.* Journal of magnetism and magnetic materials, 2010. **322**(2): p. 208-213.

4. Kim, S.J., et al., *Superparamagnetic iron oxide nanoparticles for direct labeling of stem cells and in vivo MRI tracking.* Contrast media & molecular imaging, 2016. **11**(1): p. 55-64.

5. Schutt, W., et al., *Applications of magnetic targeting in diagnosis and therapy--possibilities and limitations: a mini-review.* Hybridoma, 1997. **16**(1): p. 109-17.

6. Olsvik, O., et al., *Magnetic separation techniques in diagnostic microbiology.* Clin Microbiol Rev, 1994. **7**(1): p. 43-54.

7. Valenzuela, R., et al., *Influence of stirring velocity on the synthesis of magnetite nanoparticles (Fe3O4) by the co-precipitation method.* Journal of Alloys and Compounds, 2009. **488**(1): p. 227-231.

8. Gupta, A.K. and A.S.G. Curtis, *Lactoferrin and ceruloplasmin derivatized superparamagnetic iron oxide nanoparticles for targeting cell surface receptors.* Biomaterials, 2004. **25**(15): p. 3029-3040.

9. Laurent, S., et al., *Magnetic iron oxide nanoparticles: synthesis, stabilization, vectorization, physicochemical characterizations, and biological applications.* Chemical reviews, 2008. **108**(6): p. 2064-2110.

10. Gribanov, N., et al., *Physico-chemical regularities of obtaining highly dispersed magnetite by the method of chemical condensation.* Journal of Magnetism and Magnetic Materials, 1990. **85**(1-3): p. 7-10.

11. Xia, T., et al., *Novel complex-coprecipitation route to form high quality triethanolamine-coated Fe 3 O 4 nanocrystals: their high saturation magnetizations and excellent water treatment properties.* CrystEngComm, 2012. **14**(18): p. 5741-5744.

12. Majewski, P. and B. Thierry, *Functionalized Magnetite Nanoparticles - Synthesis, Properties, and Bio-Applications.* Critical Reviews in Solid State and Material Sciences, 2007. **32**: p. 203-215.

13. Torchilin, V.P. and V.S. Trubetskoy, *Which polymers can make nanoparticulate drug carriers long-circulating?* Advanced drug delivery reviews, 1995. **16**(2-3): p. 141-155.

14. Kim, D.K., et al., *Protective coating of superparamagnetic iron oxide nanoparticles.* Chemistry of Materials, 2003. **15**(8): p. 1617-1627.

15. Herrmann, J. and R. Bodmeier, *Biodegradable, somatostatin acetate containing microspheres prepared by various aqueous and non-aqueous solvent evaporation methods.* European Journal of Pharmaceutics and Biopharmaceutics, 1998. **45**(1): p. 75-82.

16. Lin, S.-Y., L.-T. Ho, and H.-L. Chiou, *Microencapsulation and Controlled Release of Insulin from Polylactic Acid Microcapsules.* 1985. **13**(3): p. 187-201.

17. Kallinteri, P., et al., *Novel functionalized biodegradable polymers for nanoparticle drug delivery systems.* Biomacromolecules, 2005. **6**(4): p. 1885-94.

18. Puri, S., et al., *Drug incorporation and release of water soluble drugs from novel functionalised poly(glycerol adipate) nanoparticles.* Journal of Controlled Release, 2008. **125**(1): p. 59-67.

19. Taresco, V., et al., *Properties of acyl modified poly (glycerol-adipate) comb-like polymers and their self-assembly into nanoparticles.* Journal of Polymer Science Part A: Polymer Chemistry, 2016. **54**(20): p. 3267-3278.

20. Taresco, V., et al., *New N-acyl amino acid-functionalized biodegradable polyesters for pharmaceutical and biomedical applications.* RSC Advances, 2016. **6**(111): p. 109401-109405.

21. Suksiriworapong, J., et al., *Synthesis and properties of a biodegradable polymer-drug conjugate: Methotrexate-poly (glycerol adipate).* Colloids and Surfaces B: Biointerfaces, 2018. **167**: p. 115-125.

22. Kallinteri, P., et al., *Novel functionalized biodegradable polymers for nanoparticle drug delivery systems.* Biomacromolecules, 2005. **6**(4): p. 1885-1894.

23. Taresco, V., et al., *Variation in structure and properties of poly (glycerol adipate) via control of chain branching during enzymatic synthesis.* Polymer, 2016. **89**: p. 41-49.

24. Kresse M, W.S., Pfefferer D, Lawaczeck R, Elste V, Semmler W., *Targeting of ultrasmall superparamagnetic iron oxide (USPIO) particles to tumor cells in vivo by using transferrin receptor pathways.* Magn Reson Med., 1998. **40**(2): p. 236-242.

25. Fessi, H., et al., *Nanocapsule formation by interfacial polymer deposition following solvent displacement.* International journal of pharmaceutics, 1989. **55**(1): p. R1-R4.

26. Sun, Z., et al., *Characterization of cellular uptake and toxicity of aminosilane-coated iron oxide nanoparticles with different charges in central nervous system-relevant cell culture models.* International journal of nanomedicine, 2013. **8**: p. 961.

27. Wang, Y.-X.J., S.M. Hussain, and G.P. Krestin, *Superparamagnetic iron oxide contrast agents: physicochemical characteristics and applications in MR imaging.* European radiology, 2001. **11**(11): p. 2319-2331.

28. Meng, W., et al., *Uptake and metabolism of novel biodegradable poly (glycerol-adipate) nanoparticles in DAOY monolayer.* Journal of controlled release, 2006. **116**(3): p. 314-321.

29. Kang, Y., et al., *Synthesis and Characterization of Nanometer-Size Fe3O4 and γ-Fe2O3 Particles.* Chemistry of Materials, 1996. **8**(9): p. 2209-2211.

30. Veiseh, O., J.W. Gunn, and M. Zhang, *Design and fabrication of magnetic nanoparticles for targeted drug delivery and imaging.* Advanced drug delivery reviews, 2010. **62**(3): p. 284-304.

31. Arias, J.L., et al., *Magnetite/poly (alkylcyanoacrylate)(core/shell) nanoparticles as 5-Fluorouracil delivery systems for active targeting.* European journal of pharmaceutics and biopharmaceutics, 2008. **69**(1): p. 54-63.

32. Prozorov, T., et al., *Effect of surfactant concentration on the size of coated ferromagnetic nanoparticles.* Thin Solid Films, 1999. **340**(1-2): p. 189-193.

33. Arias, J.L., et al., *Magnetite/poly(alkylcyanoacrylate) (core/shell) nanoparticles as 5-Fluorouracil delivery systems for active targeting.* Eur J Pharm Biopharm, 2008. **69**(1): p. 54-63.

34. Riley, T., et al., *Colloidal stability and drug incorporation aspects of micellar-like PLA-PEG nanoparticles.* Colloids and Surfaces B: Biointerfaces, 1999. **16**(1-4): p. 147-159.

35. Rotureau, E., et al., *Application of amphiphilic polysaccharides as stabilizers in direct and inverse free-radical miniemulsion polymerization.* Colloids and Surfaces A: Physicochemical and Engineering Aspects, 2008. **331**(1-2): p. 84-90.

36. Barrera, C., A.P. Herrera, and C. Rinaldi, *Colloidal dispersions of monodisperse magnetite nanoparticles modified with poly(ethylene glycol).* Journal of Colloid and Interface Science, 2009. **329**(1): p. 107-113.

37. Ahmad, T., et al., *Particle size dependence of relaxivity for silica-coated iron oxide nanoparticles.* Current Applied Physics, 2012. **12**(3): p. 969-974.

38. Duan, H., et al., *Reexamining the effects of particle size and surface chemistry on the magnetic properties of iron oxide nanocrystals: new insights into spin disorder and proton relaxivity.* The Journal of Physical Chemistry C, 2008. **112**(22): p. 8127-8131.

39. Tong, S., et al., *Coating optimization of superparamagnetic iron oxide nanoparticles for high T2 relaxivity.* Nano letters, 2010. **10**(11): p. 4607-4613.

Supplementary information

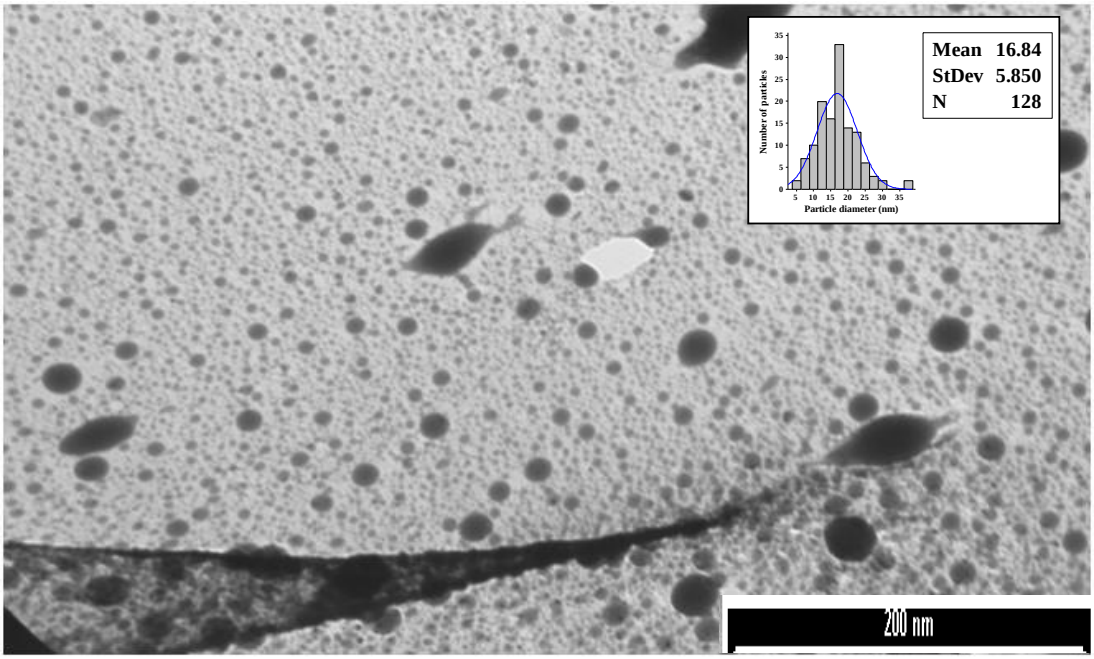

Figure S1: TEM image of IONPs coated with PGA 0% (0.2 mg) in of acetone (2 ml). Showing fewer large particles, many very small particles (Average size 16 ± 5 nm) (Scale bar 200nm).

Size analysis of Coated IONPs prepared by method 2

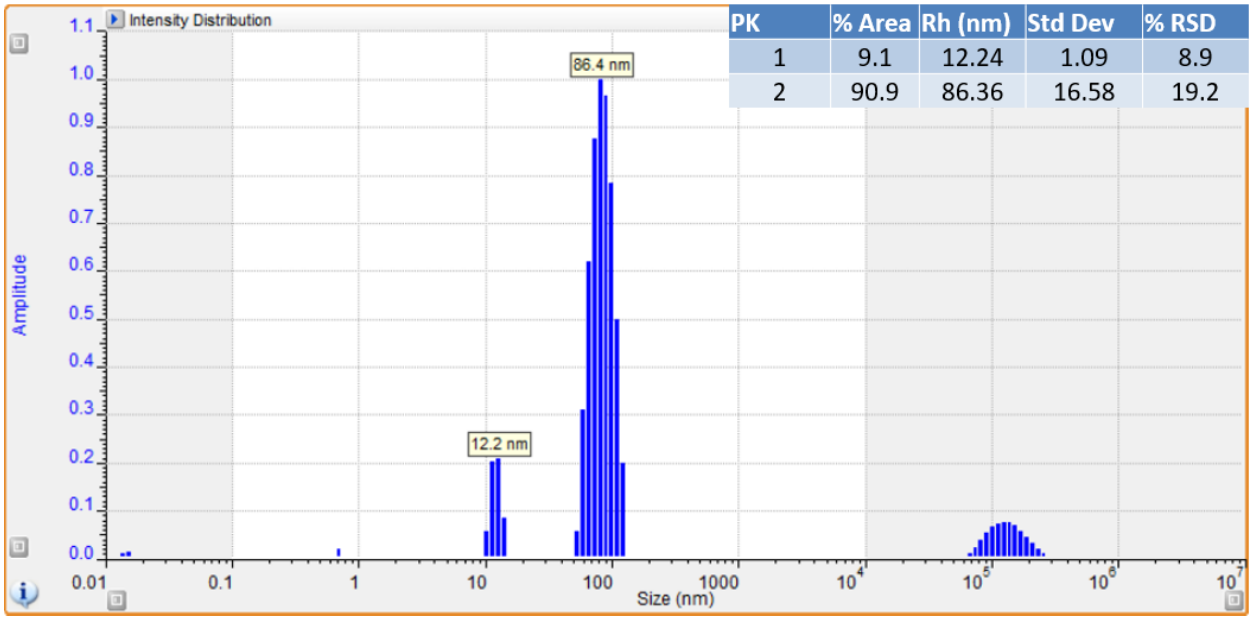

Figure S2.1: The particle size distribution of 0.05 mg PGA 40%C_8 IONPs (2 ml of acetone).

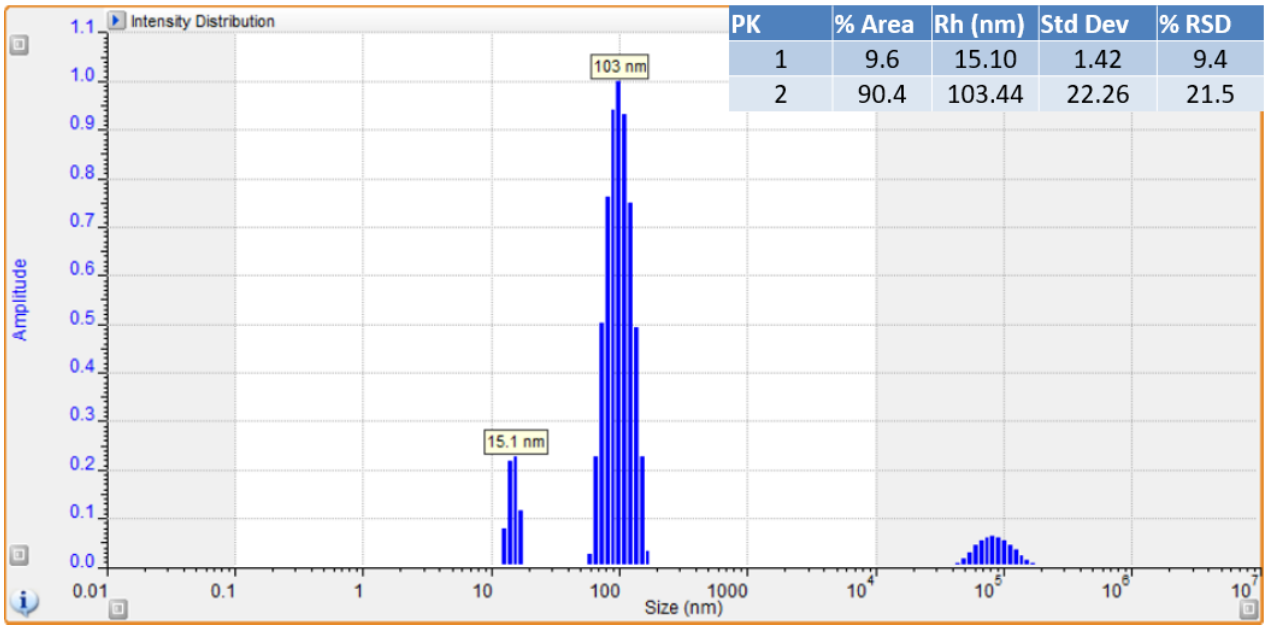

Figure S2.2: The particle size distribution of 0.1 mg PGA 40%C_8 IONPs (2 ml of acetone).

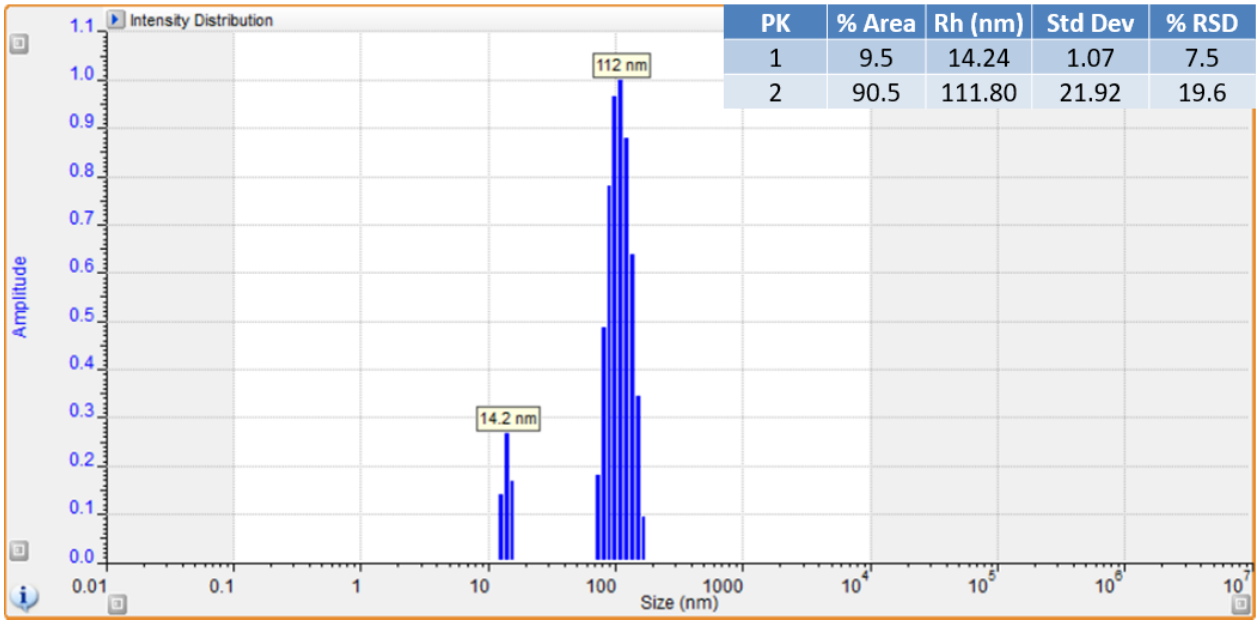

Figure S2.3: The particle size distribution of 0.2 mg PGA 40%C_8 IONPs (2 ml of acetone).

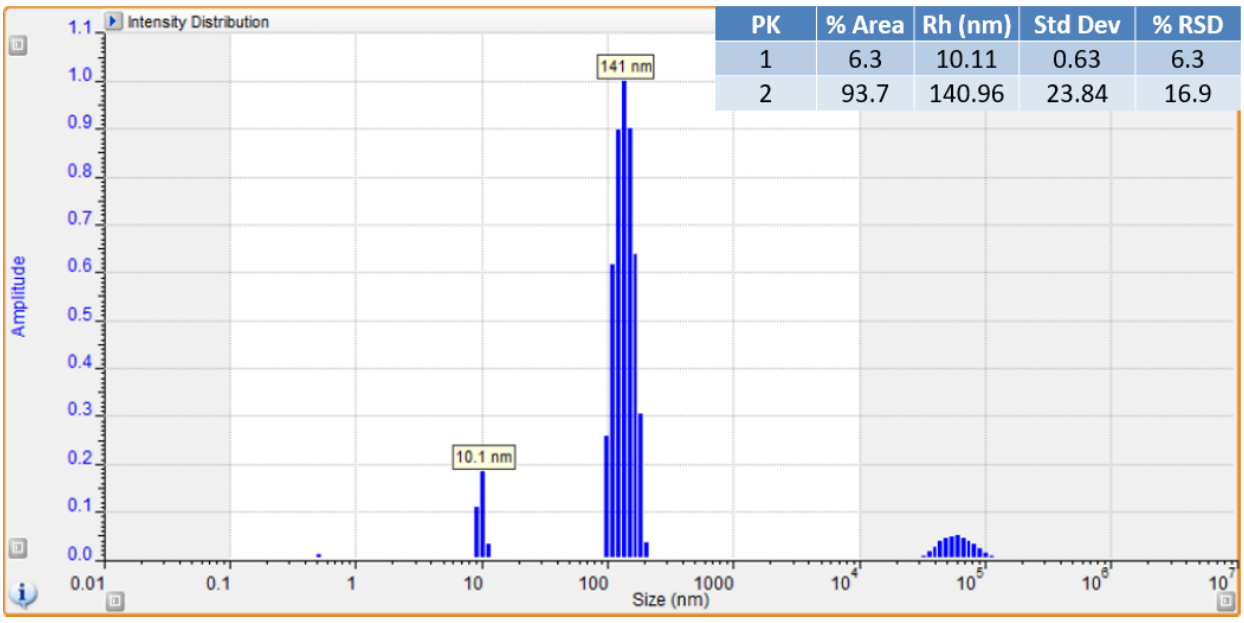

Figure S2.4: The particle size distribution of 0.3 mg PGA 40%C_8 IONPs (2 ml of acetone).

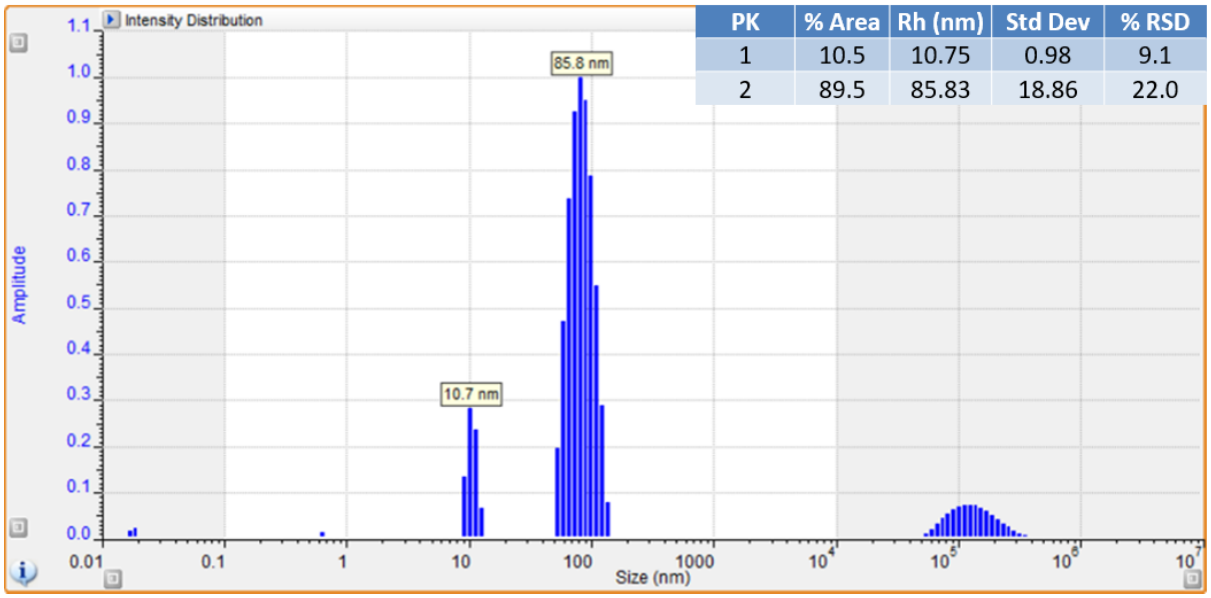

Figure S3.1: The particle size distribution of 0.05 mg PGA40%C_{18} IONPs (2 ml of acetone).

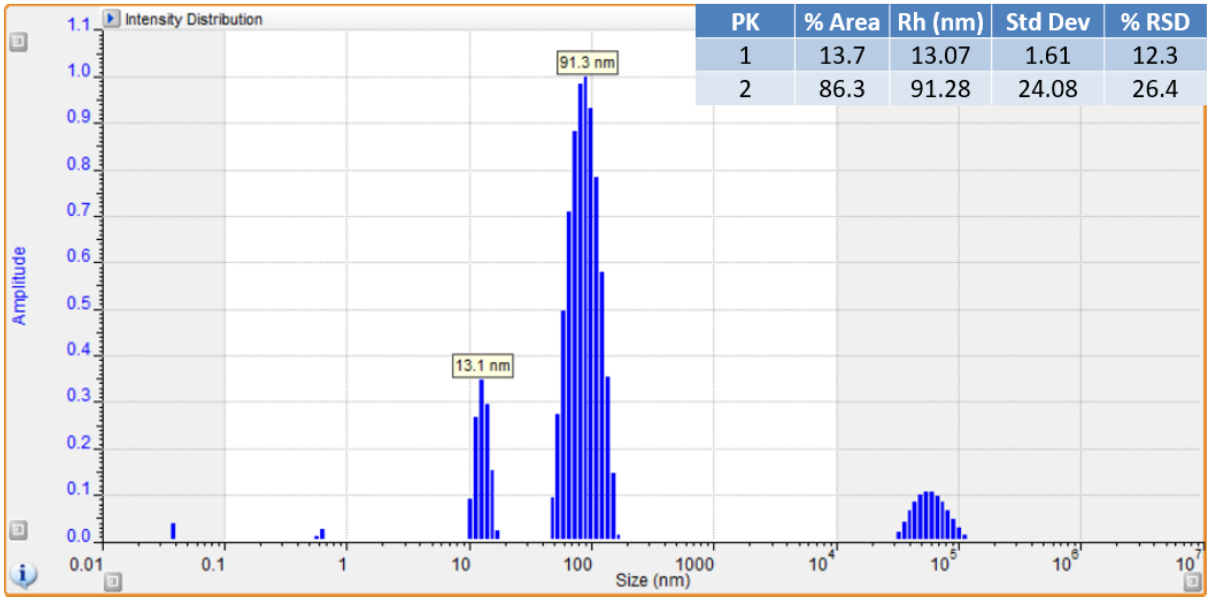

Figure S3.2: The particle size distribution of 0.1 mg PGA40% C_{18} IONPs (2 ml of acetone).

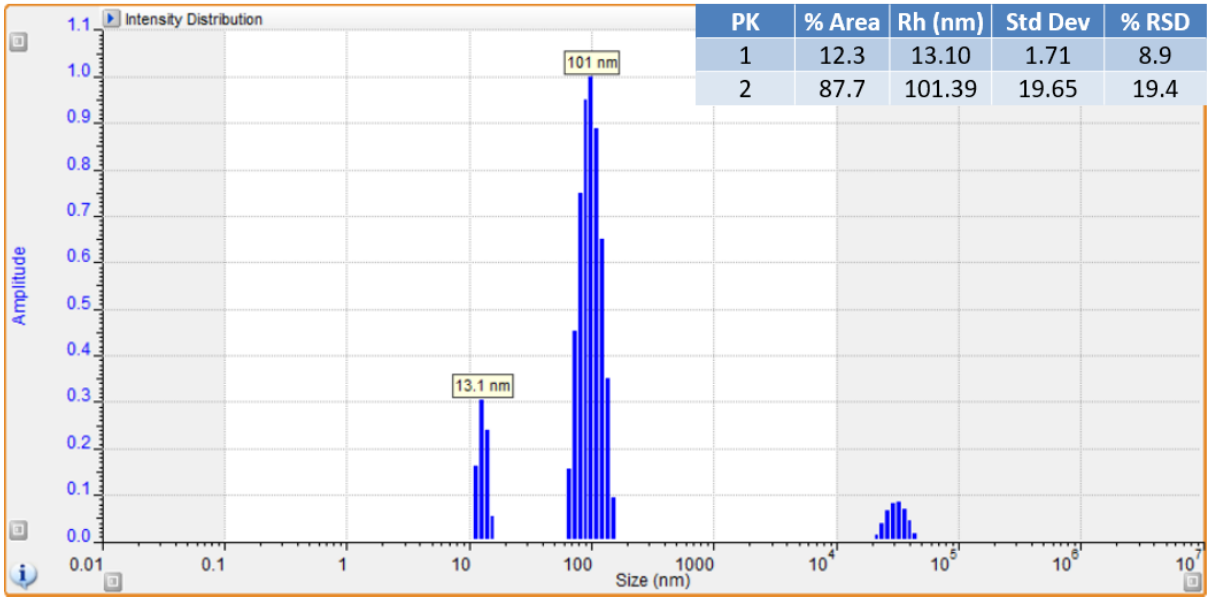

Figure S3.3: The particle size distribution of 0.2 mg PGA40%C_{18} IONPs (2 ml of acetone).

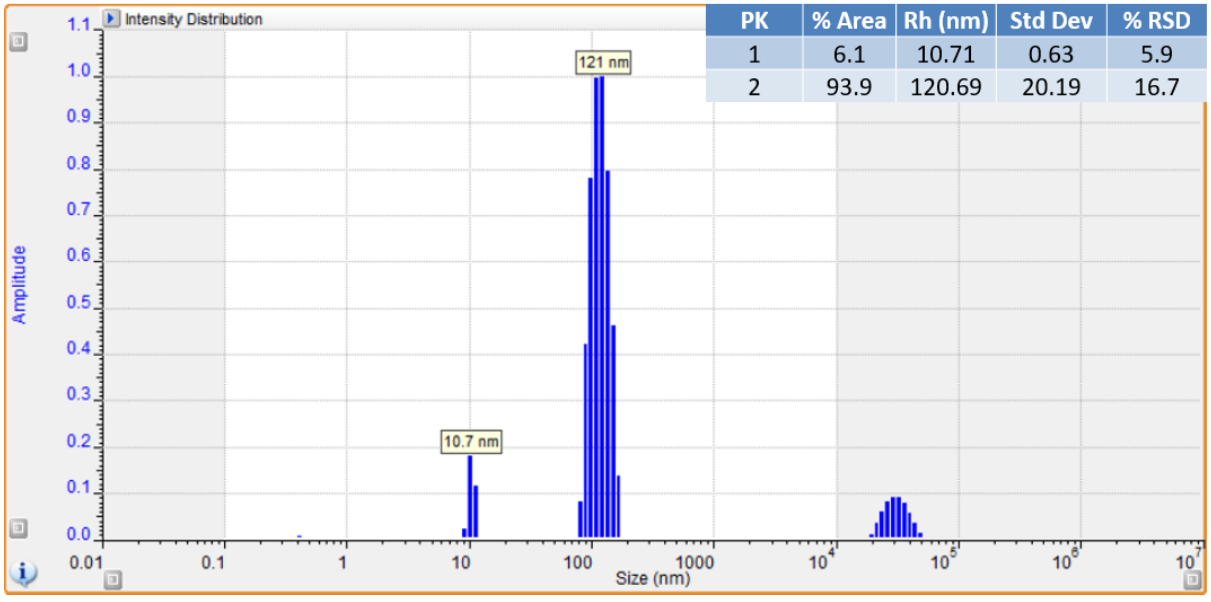

Figure S3.4: The particle size distribution of 0.3 mg PGA40%C_{18} IONPs (2 ml of acetone).

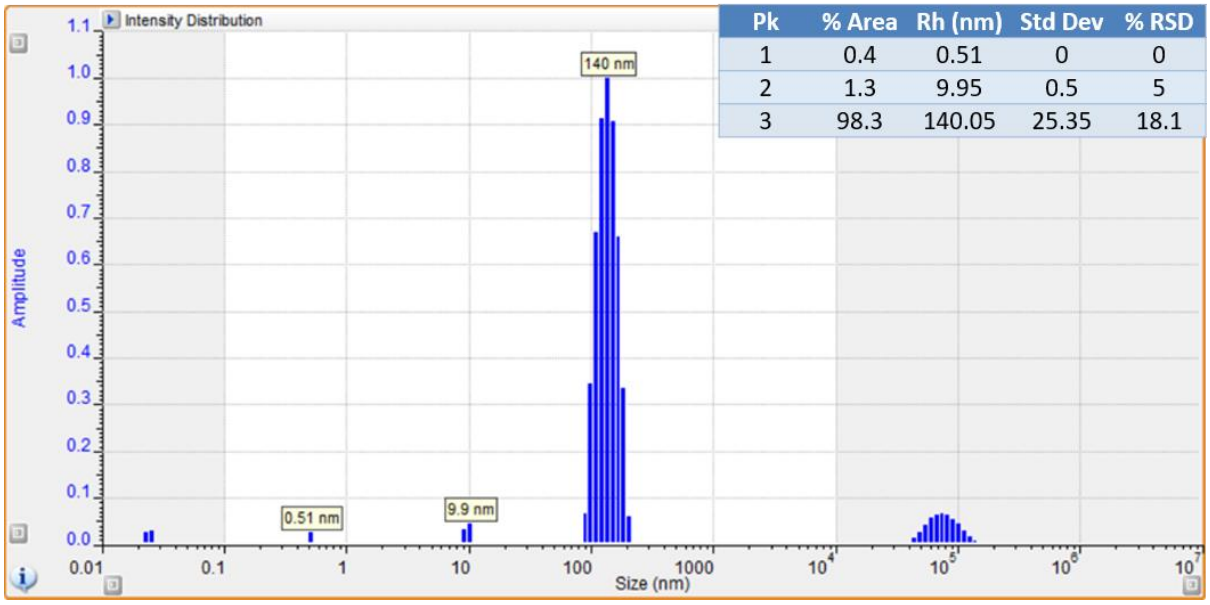

Figure S4.1: The particle size distribution of 0.025 mg PEG-PGA-SA IONPs (2 ml of acetone).

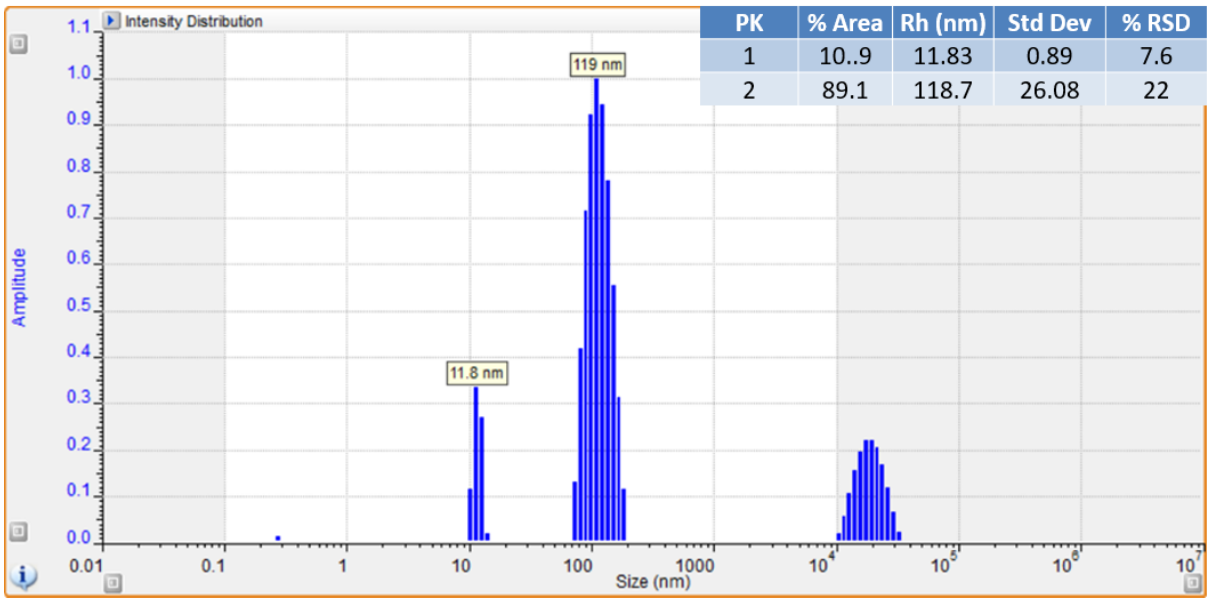

Figure S4.2: The particle size distribution of 0.05 mg PEG-PGA-SA IONPs (2 ml of acetone).

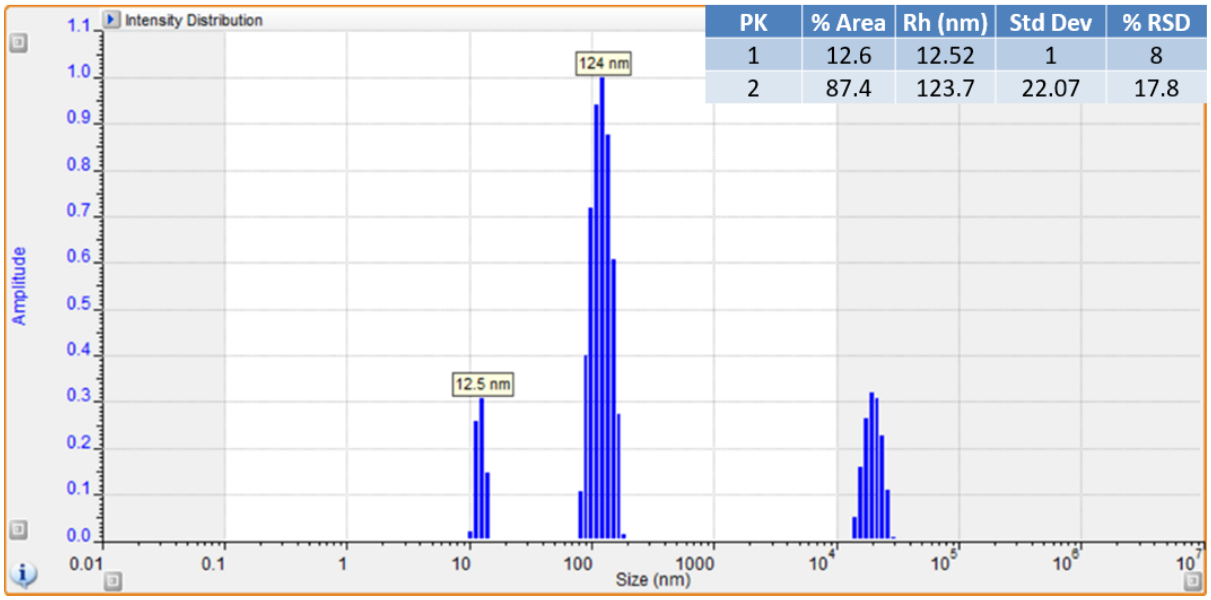

Figure S4.3: The particle size distribution of 0.1 mg PEG-PGA-SA IONPs (2 ml of acetone).

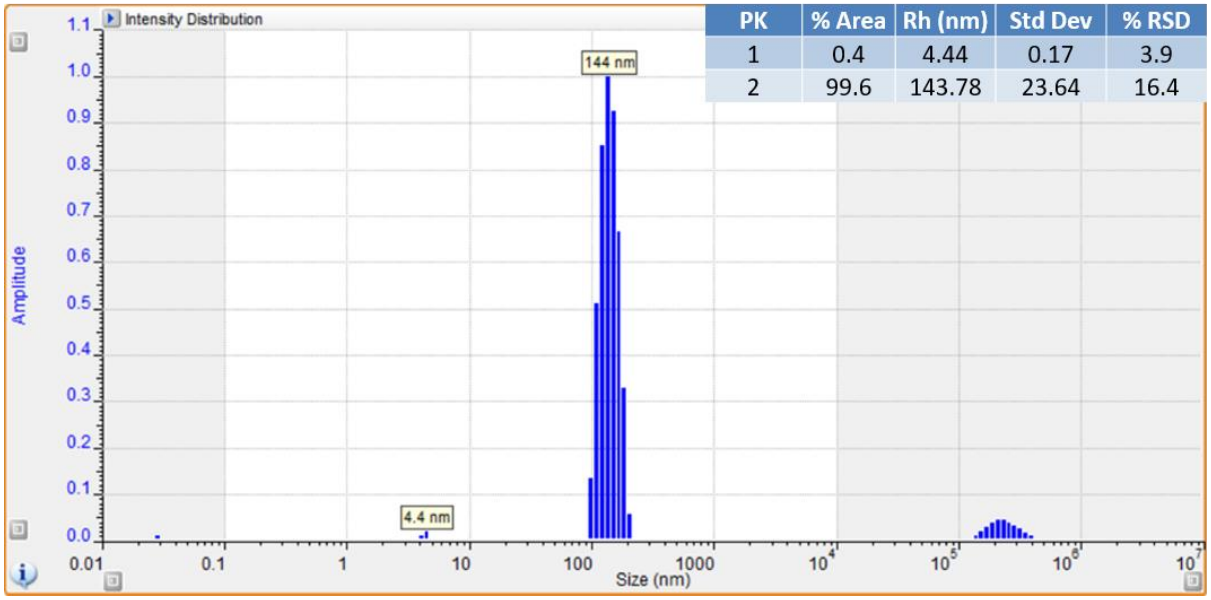

Figure S4.4: The particle size distribution of 0.2 mg PEG-PGA-SA IONPs (2 ml of acetone).

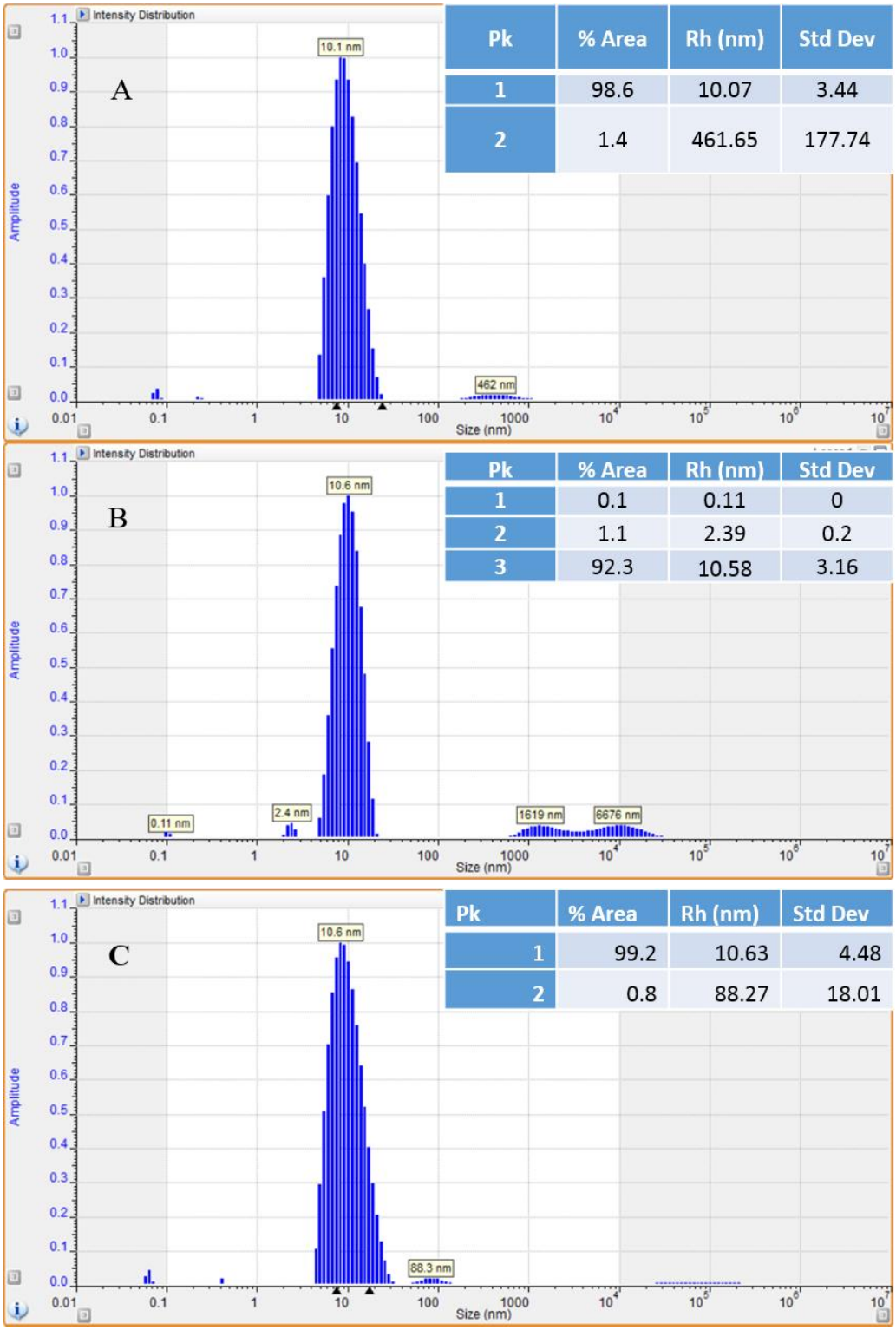

Figure S5: The hydrodynamic radii (Rh) intensity of PEGylated PGA 40% C_{18} coated IONPs by DLS. NPs of radius 10 nm were coated with different amount of polymer using interfacial deposition method where (A) 0.1 mg (B) 0.2 mg and (C) 0.3 mg PEGylated PGA 40% C_{18}. NP suspension was diluted with ultrapure water to an appropriate concentration to give 300-600 kcps. The Rh of each sample is expressed as the mean particle hydrodynamic radii ± standard deviation of 10 readings.

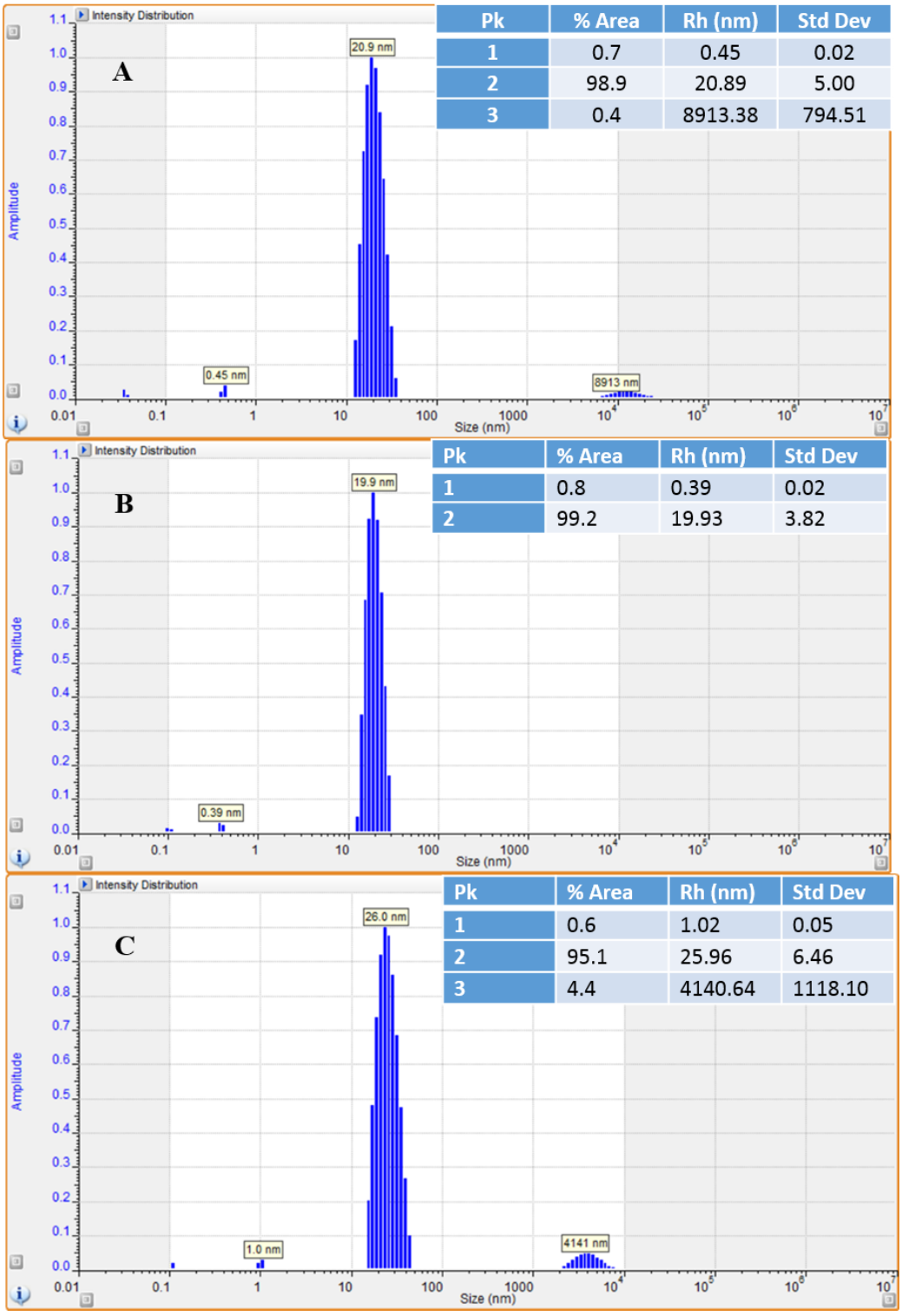

Figure S6: The hydrodynamic radii (Rh) intensity of PEGylated PGA 40%C_{18} coated IONPs by DLS. NPs of radius 18 nm were coated with different amount of polymer using interfacial deposition method where (A) 0.05 mg (B) 0.1 mg and (C) 0.2 mg PEGylated PGA 40% C_{18}. NP suspension was diluted with ultrapure water to an appropriate concentration to give 300-600 kcps. The Rh of each sample is expressed as the mean particle hydrodynamic radii ± standard deviation of 10 readings.

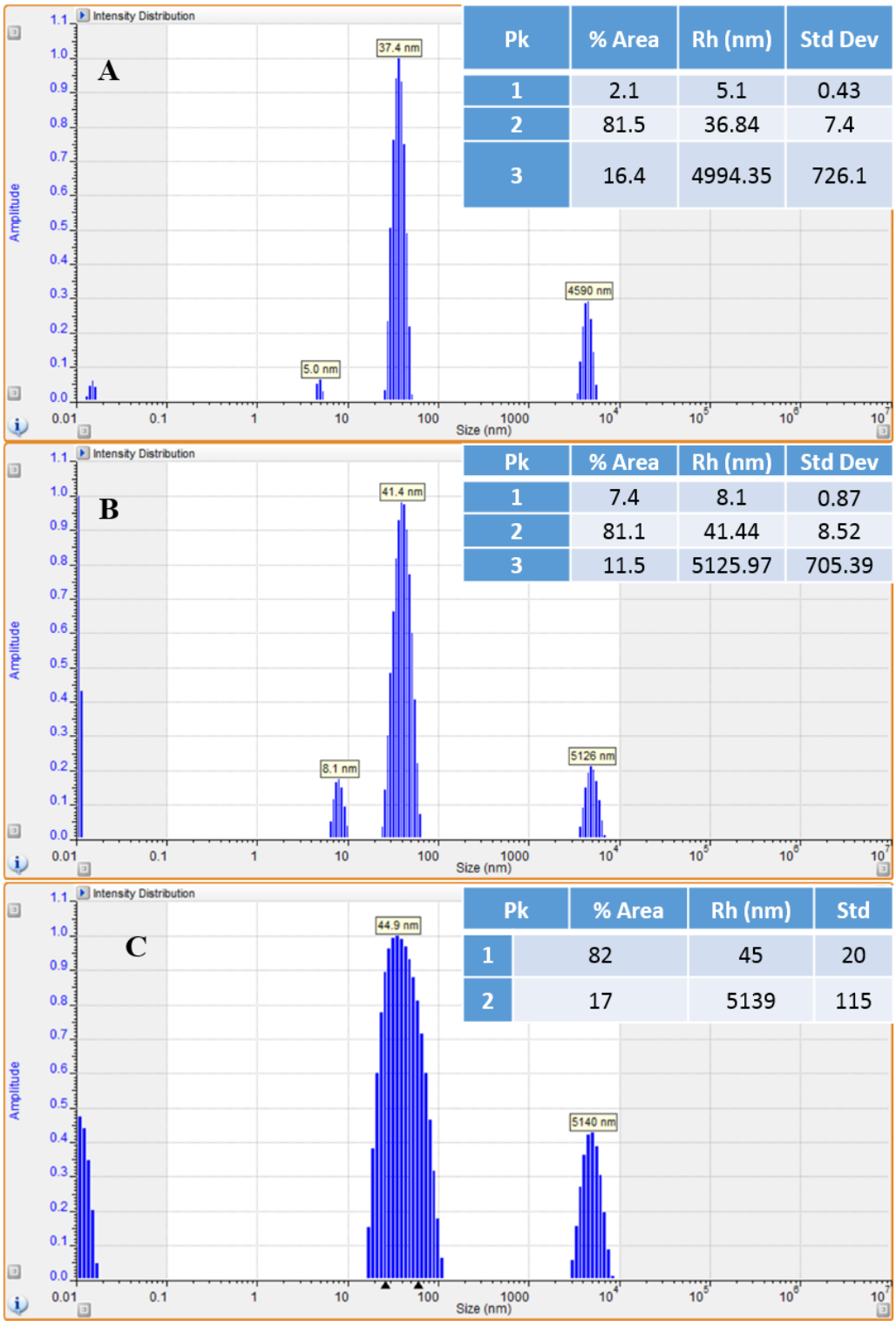

Pk	% Area	Rh (nm)	Std Dev
1	2.1	5.1	0.43
2	81.5	36.84	7.4
3	16.4	4994.35	726.1

Pk	% Area	Rh (nm)	Std Dev
1	7.4	8.1	0.87
2	81.1	41.44	8.52
3	11.5	5125.97	705.39

Pk	% Area	Rh (nm)	Std
1	82	45	20
2	17	5139	115

Figure S7: The hydrodynamic radii (Rh) intensity of PEGylated PGA 40% C_{18} coated IONPs by DLS. NPs of radius 25 nm were coated with different amount of polymer using interfacial deposition method where (A) 0.05 mg (B) 0.1 mg and (C) 0.2 mg PEGylated PGA 40% C_{18}. NP suspension was diluted with ultrapure water to an appropriate concentration to give 300-600 kcps. The Rh of each sample is expressed as the mean particle hydrodynamic radii ± standard deviation of 10 readings.

A

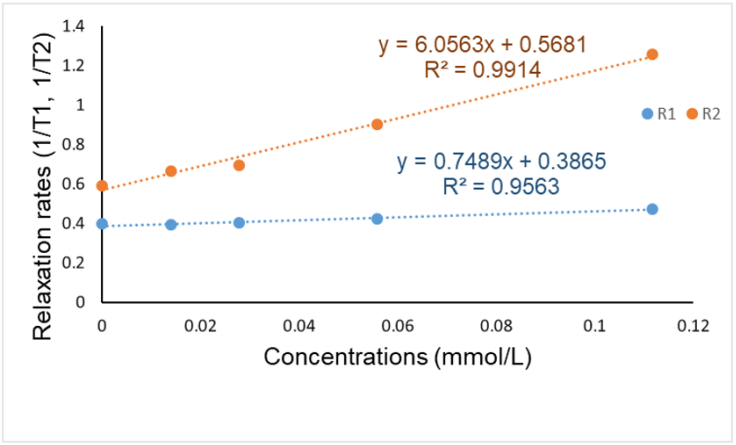

B

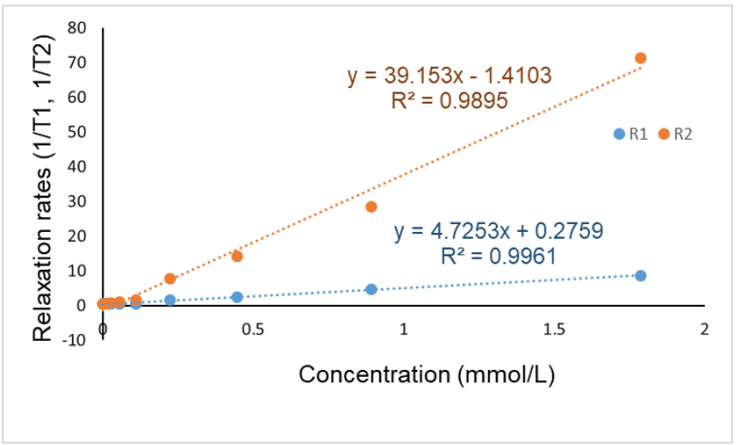

C

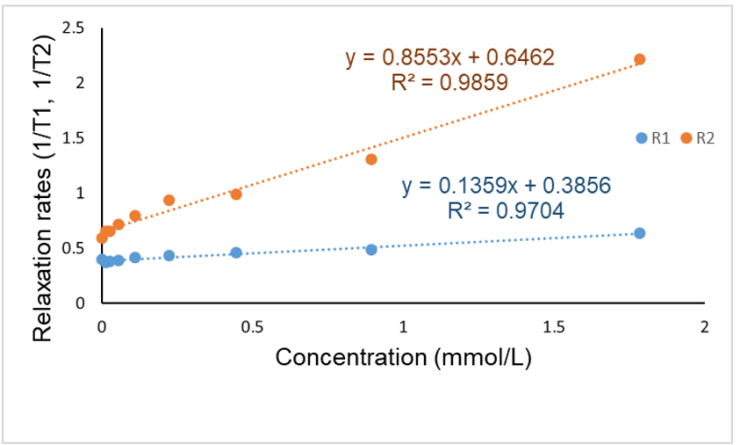

Figure S8: Plot of the proton relaxation rates (1/T1) and (1/T2) of water suspensions of polymer coated IONPs at various Iron concentrations versus the corresponding concentrations for samples A (22 nm), B (50 nm), and C (80 nm).